



Ramos-Soriano, J., Ghirardello, M., & Galan, M. C. (2021). Recent advances in multivalent carbon nanoform-based glycoconjugates. *Current Medicinal Chemistry*. Advance online publication. <https://doi.org/10.2174/0929867328666210714160954>

Peer reviewed version

Link to published version (if available):  
[10.2174/0929867328666210714160954](https://doi.org/10.2174/0929867328666210714160954)

[Link to publication record on the Bristol Research Portal](#)  
PDF-document

This is the author accepted manuscript (AAM). The final published version (version of record) is available online via Bentham Science Publishers at <https://www.eurekaselect.com/194789/article> . Please refer to any applicable terms of use of the publisher.

## University of Bristol – Bristol Research Portal

### General rights

This document is made available in accordance with publisher policies. Please cite only the published version using the reference above. Full terms of use are available: <http://www.bristol.ac.uk/red/research-policy/pure/user-guides/brp-terms/>

## Recent advances on multivalent carbon nanoform-based glycoconjugates

Javier Ramos-Soriano,<sup>a,b,†\*</sup> Mattia Ghirardello,<sup>a,‡</sup> M Carmen Galan<sup>a\*</sup>

<sup>a</sup>*School of Chemistry, University of Bristol, Cantock's Close, Bristol BS8 ITS, UK.*

<sup>b</sup>*Glycosystems Laboratory, Instituto de Investigaciones Químicas (IIQ), CSIC and Universidad de Sevilla, Américo Vespucio, 49, 41092 Sevilla, Spain.*

*E-mail: [javiramossoriano@gmail.com](mailto:javiramossoriano@gmail.com), [m.c.galan@bristol.ac.uk](mailto:m.c.galan@bristol.ac.uk)*

<sup>‡</sup> These authors contributed equally.

### **Abstract:**

Multivalent carbohydrate-mediated interactions are key to many biological processes including disease mechanisms. In order to study these important glycan-mediated interactions at a molecular level, carbon nanoforms such as fullerenes, carbon nanotubes or graphene and their derivatives have been identified as promising biocompatible scaffolds that can mimic the multivalent presentation of biologically relevant glycans. In this minireview we will summarize the most relevant examples of the last few years in the context of their applications.

### **1. Introduction.**

Carbohydrates are ubiquitous and heterogeneous molecules which are fundamental to many biological processes that build and sustain life.<sup>1</sup> These include a myriad of relevant biological, physiological as well as pathological events, such as cell growth and differentiation, pathogen infection, tumor progression and metastasis, inflammation, and many others.<sup>2</sup> These carbohydrate-mediated processes result from interactions with specific receptors, mainly proteins known as lectins.<sup>3</sup> Carbohydrate–lectin interactions are often characterized by high selectivity and low affinity (typically in the mM to  $\mu$ M range) and in most cases require divalent cations (e.g. calcium). Nature compensates this low affinity by employing multivalent interactions resulting from the presentation of multiple copies of the carbohydrate epitopes and receptors, this effect is often referred to as multivalency.<sup>4, 5</sup> These type of interactions allow the increase of both affinity and selectivity of the binding process, however, from the molecular point of view, the nature of this increment of affinity in multivalency is not completely understood due to the enormous complexity of this process. In fact, it is assumed that clustering, rebinding, chelation, etc. can all contribute simultaneously to the multivalent interaction, and dissecting the weight of each component separately is in most cases not possible.<sup>6</sup> For these reasons and because of how important the fundamental understanding of protein-carbohydrate mediated processes is, the study of multivalent interactions is the topic of much research in the glycobiology field.

In order to gain better insights of multivalent carbohydrate-mediated processes and their interactions with their corresponding receptors, surface functionalization of nanomaterials with different glycan has been exploited as a synthetic strategy and a wide range of novel nanoprobe that can present glycans in different multivalent 3D arrangements have been designed.<sup>7</sup> Indeed, some of these multivalent architectures bearing carbohydrate ligands have been evaluated toward enzymatic interactions studies,<sup>8</sup> drug delivery applications and in the development of anticancer therapies.<sup>9, 10</sup> Not only multivalency, but also the shape and size of the probe, the nature of the surface coating and type of functionalization (e.g. conjugating

linker), play a pivotal role in the interaction of these materials with their biological target and thus it will influence both their *in vitro* and *in vivo* activity. In the search for innovative multivalent platforms, several authors have focused on less unexplored carbon nanostructures, such as fullerenes, nanotubes or graphene and their derivatives, as very attractive, promising and biocompatible 2D or 3D scaffolds for the multivalent presentation of sugars. All these multivalent carbon nanoform-based glycoconjugates will be discussed in this review, with an emphasis in their biological applications in the last recent years.

## 2. Glycofullerenes.

Among the many bioactive carbon nanoforms developed during the last few years, glycofullerenes are of particular interest. Particularly, in the search for innovative multivalent scaffolds, hexa-substituted glycofullerenes have attracted much attention owing to its octahedral symmetry and globular structure, which allow the 3D distribution of the sugars around the C<sub>60</sub> core and make these scaffolds an interesting biocompatible carbon nanoplatform for the multivalent presentation of carbohydrates.<sup>11, 12</sup> Moreover, [60]fullerene post-functionalizable hexakis-adducts allow the simultaneous grafting of twelve groups which offers a clear advantage for the fast construction of dendrimers with regard to other carbon-based platforms in which multivalent conjugation is much less defined.<sup>13</sup>

### 2.1. Glycofullerenes as antiviral agents.

One of the many strategies aimed to design glycoconjugates as antiviral agents against viral infections is based on the development of probes that mimic the carbohydrate cloak on the viral surface (generally of globular geometry) which can interfere with the infectious process by blocking the interaction with the corresponding cell-surface receptor. Within this context, glycofullerenes have been remarkably exploited during the last decade for the preparation of multivalent glycoconjugates.<sup>14, 15</sup>

Rojo, Martin, Delgado *et al.* have developed a straightforward strategy based on the Copper (I)-Catalyzed Alkyne-Azide Cycloaddition (CuAAC) reaction to “click” simultaneously twelve glycoderivative-motifs to alkyne-substituted hexakis-adducts in a regioselective and efficient way and in few steps with good yields.<sup>16-18</sup> In particular, their attention have been focused on the development of sugar-balls to inhibit viral infections of emergent viruses such as Ebola (EBOV), Zika (ZIKV) and Dengue (DENV). It is known that these kinds of viruses interact with DC-SIGN receptor, a C-type lectin present on the surface of immune cells.<sup>19-22</sup> The main carbohydrate ligand recognized by DC-SIGN is the high-mannose glycan with the mannosyl nonasaccharide Man<sub>9</sub> being the main epitope to interact with this receptor.<sup>23</sup> In 2016, the authors described the preparation of tridecafullerenes **1-3** (Figure 1), so-called ‘superballs’,<sup>24</sup> in order to dramatically increase the valency and the size of the fullerene derivatives, using a synthetic strategy they had previously reported.<sup>16-18</sup> These superballs were coated with 120 peripheral mannose subunits, which were constituted by a central C<sub>60</sub> scaffold in which the 12 alkyne groups were clicked to 12 mannose-containing C<sub>60</sub> units. The synthesis of these superballs was performed in good yields of 73-79% via CuAAC click reaction employing CuBr·S(CH<sub>3</sub>)<sub>2</sub> as the catalyst and sodium ascorbate as the reducing agent in presence of a piece of metallic Cu in DMSO.

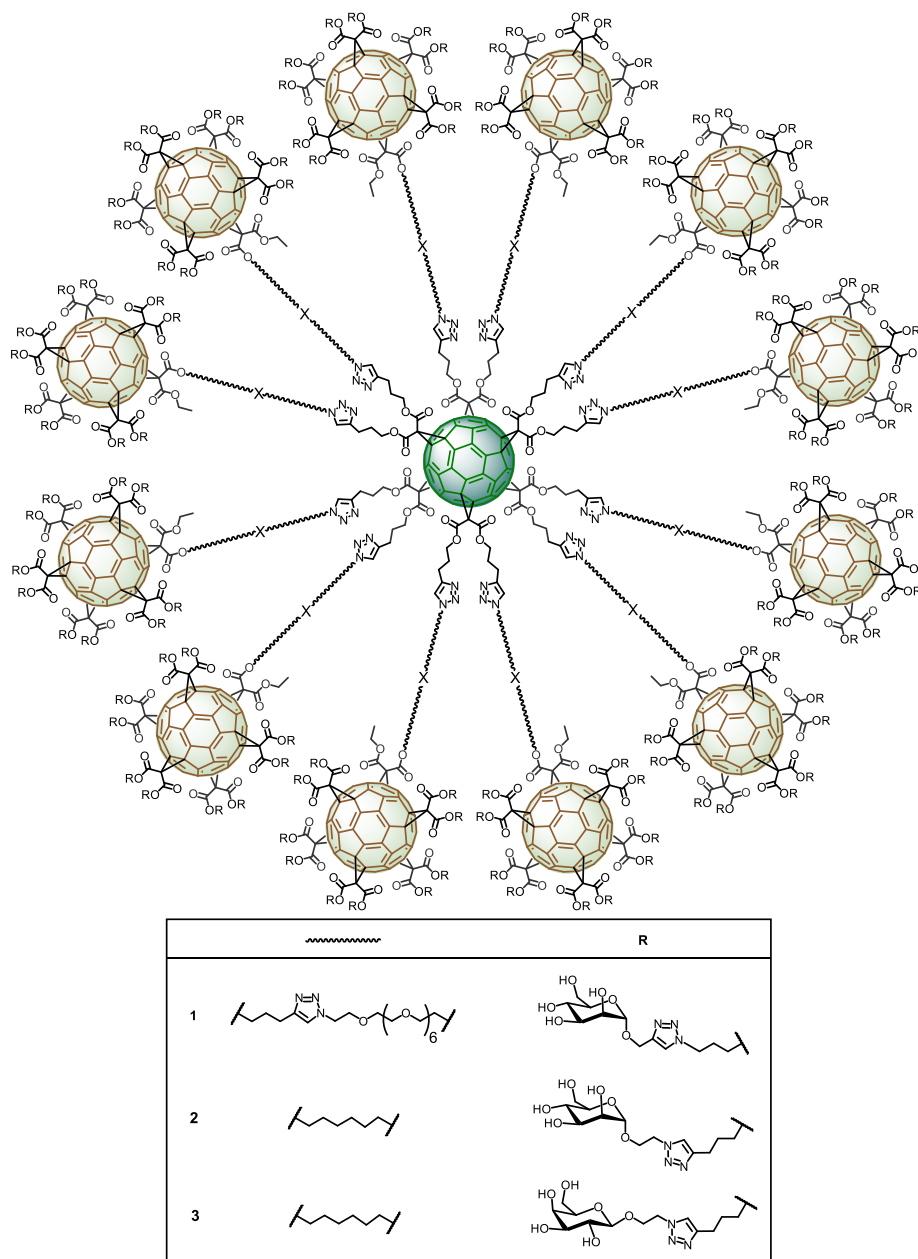


**Figure 1.** General structures of superballs **1-3**.

Although all tridecafullerenes contain the same number of sugars, in order to study the effect of the steric congestion on antiviral properties, two different linkers were used to obtain final products with different spacers between the peripheral sugar-functionalized fullerenes and the fullerene central core. The most flexible ethylene glycol-based linker could allow for the better accessibility and availability of the carbohydrates in the interaction with the corresponding receptor. Moreover, as negative control, a tridecafullerene coated with galactose (**3**) was also prepared, since DC-SIGN is not able to recognize galactose. In addition to those, glycofullerenes decorated with 12 and 36 mannoses were also included in these series to study the effect of multivalency presentation on the antiviral properties.<sup>18</sup>

Despite the high molecular weights and complexity of these molecules, compounds could be well characterized by standard spectroscopic techniques (FTIR and NMR

spectroscopy) as well as dynamic light scattering (DLS), transmission electron microscopy (TEM) and X-ray photoelectron spectroscopy (XPS).

The ability of these “giant” tridecafullerenes to inhibit the infection of Jurkat cells using Ebola virus glycoprotein (EBOGP) pseudotyped viral particles as infectious agents (Figure 2) was evaluated and the outcomes summarized in Table 1.

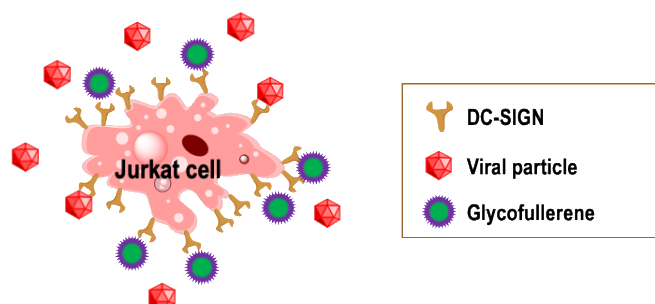


**Figure 2.** “Giant” tridecafullerenes inhibiting the Ebola virus glycoprotein (EBOGP) pseudotyped viral particles infection of Jurkat cells.

**Table 1. Comparison of IC<sub>50</sub> and RIP values of different mannosylated glycofullerenes.**

Compound	N° of Man	IC <sub>50</sub> (nM)	RIP*
<b>1</b>	120	0.667	1.58 x 10 <sup>4</sup>
<b>2</b>	120	20.375	5.2 x 10 <sup>2</sup>
<b>4</b>	36	300	1.17 x 10 <sup>2</sup>
<b>5</b>	36	68,000	0.5
<b>6</b>	12	2,000	53
<b>α-methyl-D-mannopyranoside</b>	1	1.27 x 10 <sup>6</sup>	1

\*RIP, calculated as (IC<sub>50</sub>)<sub>mono</sub>/IC<sub>50</sub>\*valency ((IC<sub>50</sub>)<sub>mono</sub>, IC<sub>50</sub> of the monovalent compound; IC<sub>50</sub>\*valency, IC<sub>50</sub> of the multivalent compound multiplied by the number of ligands present in the glycofullerene compound).

Both tridecafullerenes functionalized with mannose moieties exhibited very strong antiviral activity at picomolar to nanomolar concentration range. Compound **1** (IC<sub>50</sub> of ~0.7 nM) was almost one order of magnitude more potent at inhibiting the infection process in comparison with the most compact tridecafullerene **2** (IC<sub>50</sub> of ~20). A multivalent effect could be observed when compared with glycodendriferfullerenes coated with 36 mannoses **4** (long linker) and **5** (short linker), whose IC<sub>50</sub> were of 300 and 68000 nM, respectively. The IC<sub>50</sub> values for tridecafullerenes surpassed by three orders of magnitude (two if the mannoses number is taken in account) in comparison with glycofullerene **6** endowed with 12 mannoses. These data revealed that the valency number, as well as the length and the flexibility of the linker unit between the core and the peripheral sugars, were important factors involved in the affinity of multivalent ligands towards antiviral infections. The importance of the length of the linker in glycofullerenes in biomedical applications were previously confirmed by NMR spectroscopy studies.<sup>25</sup>

More recently, some of us have reported the synthesis of groundbreaking mannobiosylated tridecafullerenes, so-called ‘nanoballs’, with up to 360 sugar functionalities.<sup>26</sup> Interestingly, nanoballs were decorated with α(1,2)mannobiosides instead of mannose, since the presence of the disaccharides increase by 3-4 fold the affinity to DC-SIGN. In this case, the synthetic strategy employed was based on post-functionalizable hexakis adducts of [60]fullerene via metal-free click chemistry.<sup>27,28</sup> Symmetric and asymmetric hexakis-adduct of C<sub>60</sub> functionalized with twelve cyclooctyne groups were used to

further carry out the strain-promoted azide-alkyne cycloaddition (SPAAC) reaction with the corresponding azide derivative.<sup>27</sup> This methodology allowed for the efficient assembly of glycofullerenes functionalized with 12 galactoses (**8**, as negative control), 12 mannoses (**9**, as positive control) and 12 (**10**) and 36 (**11**)  $\alpha(1,2)$ mannobiosides motifs. On the other hand, the synthesis of nanoballs coated with 120 (**12**) and 360 (**13**)  $\alpha(1,2)$ mannobiosides residues was also accomplished in this manner. It is worth highlighting that the synthesis of C<sub>60</sub>-360ManMan (**13**) represents the fastest dendritic growth reported up to now in the literature. From a synthetic point of view, the SPAAC methodology offers several benefits in comparison with CuAAC version such as the absence of cytotoxic copper, easier purification, lower reaction times and higher yields. This represents a clear advantage when using sophisticated building blocks such as mannobiosides.

In a similar way, the team evaluated the inhibitory effect of these molecules in a pseudotyped Zika and Dengue viral model employing Jurkat DC-SIGN cells. First, the efficiency of compounds **8-13** to inhibit DC-SIGN was tested, showing dependence on the numbers of carbohydrates. Secondly, the antiviral activity of the three best ligands with 36 (**11**), 120 (**12**) and 360 (**13**) disaccharides (Figure 3) was measured and their IC<sub>50</sub>s values are summarized in Table 2.

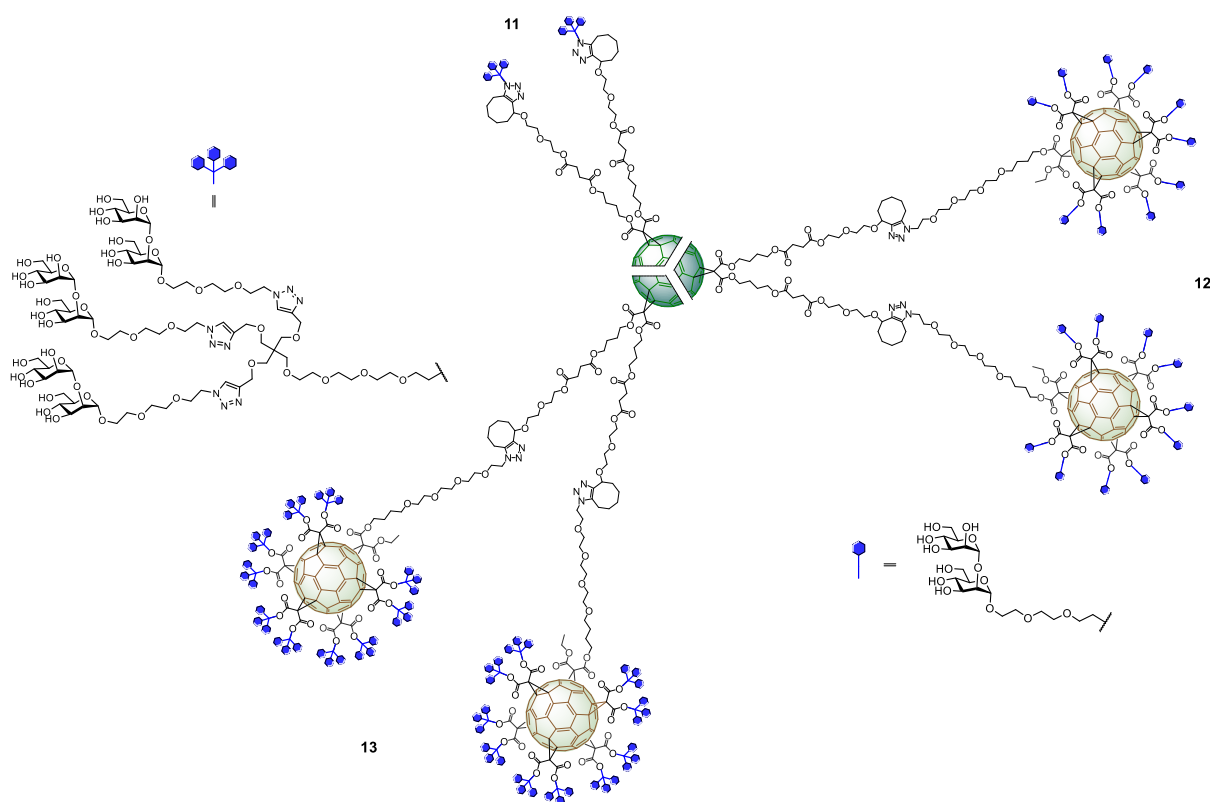


**Figure 3.** General structures of nanoballs **11-13**.

Compound	N° of Man-Man	ZIKA (IC <sub>50</sub> nM)	DENGUE (IC <sub>50</sub> nM)
<b>11</b>	36	8.35	7.71
<b>12</b>	120	0.52	0.098
<b>13</b>	360	0.067	0.035

The three nanoballs **11-13** showed very strong antiviral activity at picomolar to nanomolar concentrations, with the ligand bearing 360 sugars (**13**) being the best one to inhibit the viral infection for both ZIKV and DENV in the picomolar range (IC<sub>50</sub> of 67 pM for ZIKV and IC<sub>50</sub> of 35 pM for DENV). Enhancement of one order of magnitude was observed with the

increase of the numbers of sugars, which reveals a clear multivalent effect. These data for both super- and nanoballs suggest that an increase of valency of the systems turned out to achieve improved biological activity, validating the use of higher glycofullerene-based antivirals as effective probes to block carbohydrate receptors and inhibit the infection process.

## 2.2. Glycofullerenes as enzymatic inhibitors.

Owing to the enormous relevance of glycosidases in nature, these important carbohydrate-modifying enzymes are considered attractive targets for the development of biomedical agents for the treatment of pathologies<sup>29, 30</sup> such as viral infections,<sup>31</sup> cancer and tumour metastasis,<sup>32, 33</sup> influenza,<sup>34</sup> diabetes,<sup>35-37</sup> Alzheimer disease,<sup>38</sup> lysosomal storage disorders<sup>39</sup> and as antimicrobial agents.<sup>40, 41</sup> In this context, the search of new multivalent platforms as glycosidase inhibitor is a growing area of interest in glycoscience that has emerged a few years ago and has led to the development of inhibitors based on a wide range of core structures such as cyclodextrins,<sup>42-45</sup> glucose,<sup>46</sup> galactose,<sup>46</sup> calix[4]arene,<sup>46</sup> porphyrin,<sup>46</sup> trehalose,<sup>46</sup> micelles,<sup>47</sup> cyclopeptoid cores,<sup>48, 49</sup> dextran polymers,<sup>50</sup> nanodiamonds,<sup>51</sup> among others. Of note is the use of iminosugar-fullerene conjugates with high valence displaying strong binding enhancements over the corresponding monovalent inhibitory motif (inhitope).<sup>52-54</sup>

Mellet, Compain, Nierengarten *et al.*<sup>55-57</sup> have reported the synthesis of C<sub>60</sub>-based DNJ glycoconjugates and sp<sup>2</sup> iminosugar glycomimetics with potential ability to inhibit the activity of different glycosidases. In the present review, we will discuss the most recent developments in the synthesis of these important DNJ glycoconjugates and their applications. Glycofullerenes coated with DNJ iminosugars using the versatile CuACC strategy described above were prepared, namely fullerodendrimers **14-15**<sup>55</sup> and the superball **16**<sup>56</sup> (Figure 4). These nanoconstructs differ in the carbohydrate valency which is presented in a globular manner. As a structurally related monovalent control, DNJ iminosugar **17** and the corresponding iminosugarball **18**<sup>58</sup> decorated with 12 DNJ moieties were also included in the study for comparison.

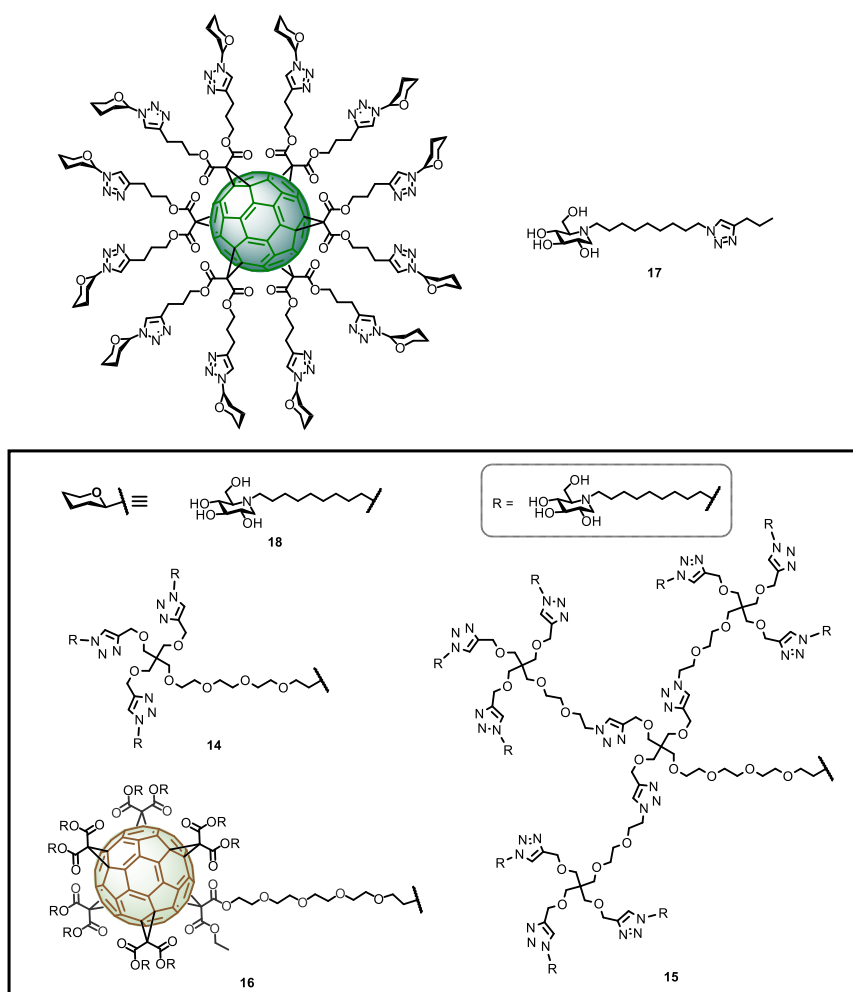


**Figure 4.** General structures of glycofullerenes **14-16** and **18** and monovalent iminosugar **17**.

The inhibition profile of the C<sub>60</sub>-based DNJ glycoconjugates **14-16** were evaluated against a panel of commercial glycosidases including  $\alpha$ -glucosidases (from yeast maltase and *A. niger* amyloglucosidases),  $\beta$ -glucosidases (from almonds),  $\alpha$ -galactosidases (from green coffee beans),  $\beta$ -galactosidase (from *E. coli*) and  $\alpha$ -mannosidases (from Jack Bean  $\alpha$ -Man). However, Mellet, Compain, Nierengarten *et al.* focused their attention on Jack Bean  $\alpha$ -Man (JB  $\alpha$ -Man), being the most popular glycosidase for multivalent enzyme inhibitory (MEI) studies. Unlike other glycosidases, JB  $\alpha$ -Man possesses open, readily accessible catalytic sites, and is highly sensitive to weak inhibitory motifs presented as multivalent glycomimetic inhibitors.<sup>3</sup> Due to this, inhibition potency enhancements well beyond that expected from a statistic effect were achieved. In this review, we discuss the results obtained from this enzyme topology. The inhibition constants ( $K_i$ ) and relative inhibition potency on a DNJ molar basis (rp/n) are summarized in Table 3.

**Table 3.**  $\alpha$ -Mannoside (JB  $\alpha$ -man) inhibitory activities ( $K_i$ ) for monovalent DNJ derivative **17** and multivalent DNJ-fullerenes **14-16** and **18**.

Compound	N° of DNJ sugar	$K_i$ ( $\mu$ M)	rp/n*
<b>14</b>	36	0.064	88
<b>15</b>	108	0.0072	262
<b>16</b>	120	0.0018	944



<b>18</b>	12	0.099	172
<b>17</b>	1	204	1

\*rp =  $K_i$  (reference)/ $K_i$  DNJ-fullerene, n = number of inhitope units relative to the number of inhitopes in the considered reference.

First, a dramatic enhancement of the glycosidase inhibitory effect was observed of three orders of magnitude for first-generation fullerodendrimer **14** as compared to that of the corresponding monovalent model compound. Moreover, this compound showed similar  $K_i$  to the corresponding dodecavalent glycocluster **18**. Second-generation fullerodendrimer **15**, with 108 DNJ motifs at the periphery, and 120-valent DNJ-coated superball **16**, behave as very potent inhibitors of JB  $\alpha$ -Man with  $K_i$  values of 7.2 and 1.8 nM, respectively. A direct comparison with the corresponding first-generation fullerodendrimer **14**, both compounds showed an additional binding enhancement of one order of magnitude. Remarkably, over a 1,000000-fold increase was observed comparing giant iminosugar ball **16** to monovalent control **17** and a 55-fold enhancement in the inhibition potency when compared to the corresponding dodecavalent version **18**, well over a statistic effect.

In order to study the effect of MEI, the relative inhibition potency on a DNJ molar basis (rp/n) was analysed. In spite of both iminosugarsballs **18** and **14** showing a similar  $K_i$ , a normalized relative inhibition potency of 172 and 88 were obtained, respectively. This feature indicated that a higher inhitope density is slightly detrimental in this case in terms of relative potency. On the other hand, the rp/n values triple in the case of the 108-valent derivative **15** when compared to the corresponding first-generation analogue **14**, showing a clearly multivalent effect. It is worth noting that the MEI effect observed for 120-valent DNJ-coated superball **16** was comparable to the 108-valent compound **15** (e.g. similar  $K_i$ ). That suggest that the inhitope density at the periphery of multivalent constructs is important, and that it also play an important role in the MEI effect. Interestingly, the inhibition activity was competitive in all cases except for **16**, where a mixed-type inhibition was observed, that is, the superiminoball can bind to both the enzyme and the enzyme-substrate complex, preventing substrate hydrolysis in both cases. The uncompetitive component reveals for the first time that strong inhibition of  $\alpha$ -mannosidase can be reached by using multivalent inhibitors even when the active site is fully occupied. It is important to highlight that this feature has only been previously observed for fullerene derivatives homogeneously decorated with carbohydrates or heterogeneously functionalized with carbohydrates and sp<sup>2</sup>-iminosugar glycomimetics<sup>59-63</sup> against  $\beta$ -galactosidase.<sup>49, 57, 64</sup>

Vicent *et al.* have extended the concept of multivalent enzyme inhibition to other major class of glycosyl processing enzymes, namely glycosyltransferases<sup>65</sup> by using multimeric glycoclusters based on fullerene as central scaffold.<sup>66, 67</sup> In 2016, they reported the synthesis of unprecedented Kdo glycofullerenes **19-22** (Figure 5) and the enzymatic assays against therapeutically relevant bacterial heptosyltransferase I (WaaC).<sup>67</sup> This transferase is an important bacterial glycosyltransferase that is involved in lipopolysaccharide biosynthesis, which catalyze the regio- and stereoselective transfer of a saccharide from a glycosyl donor to a glycan acceptor.

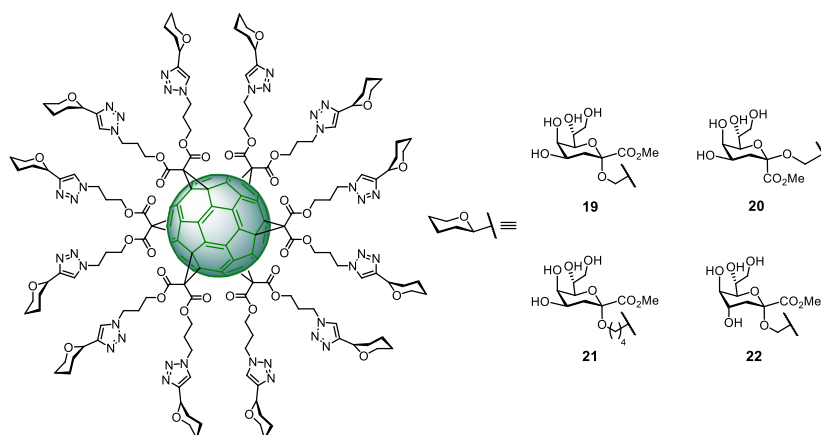


**Figure 5.** Structures of compounds **19-22**

The novel Kdo glycofullerenes displayed very potent inhibition activity in the submicromolar scale, being **19** the best inhibitor with a  $K_i = 0.14 \mu\text{M}$ . It is noteworthy that this inhibition level is rarely observed with glycosyltransferases. Moreover, they demonstrated that the inhibitory power of these glyconanomaterials depends on the absolute configuration of both C-1 and C-4 of the Kdo ligands, while the length of the spacer does not affect the affinity for WaaC. A direct comparison with the corresponding monovalent version clearly showed that no or modest multivalent effect was observed for glycofullerenes **19-22** (calculated by analysis of the affinity enhancement of a ligand when presented in a multimeric fashion, based on normalized  $\text{IC}_{50}$  values). These new discoveries have contributed to the design of a new generation of inhibitors of glycosidases employing [60]fullerene or others 3D carbon nanoforms as multivalent central core. The concept of multivalent enzyme inhibition could be applied to other kinds of enzymes which are exposed in cell or virus outer membrane.

### 2.3. Glycofullerenes as anti-bacterial agents.

Another example where [60]fullerene molecules have been employed as multivalent platform is in the field of anti-bacterial inhibition processes. In 2015, Buffet *et al.* reported the preparation of a series of water-soluble fucofullerenes **23-24** containing up to 24 fucose residues (Figure 6) against two bacterial lectins, namely LecB from *P. aeruginosa* and RSL from *R. solanacearum*.<sup>68</sup>

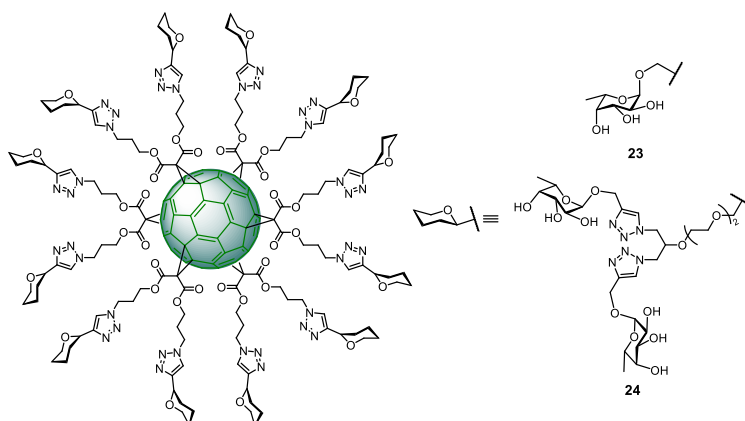


**Figure 6.** Structures of compounds **23-24**.

For both LecB and RSL, C<sub>60</sub>(Fuc)<sub>24</sub> **24** appeared to be the best inhibitor ( $K_D$  in nanomolar range, measured by ITC experiments), showing an enhancement of the binding affinity when going from monomeric to multimeric ligands. Interestingly, comparison with a monomeric reference ligand and the efficiency per ligand epitope, showed the multivalent effect was by far more important for RSL when compared to LecB. This difference could be explained in terms of topology of both lectins, being indeed completely different. While in the case of RSL, six binding pockets are located on the same face of the protein, LecB has four binding pockets located quite far apart (which means large multivalent effects might not be observed). In the latter case, it is only possible the simultaneous bind two sugar units from the same fucofullerene to two different LecB proteins. The authors concluded that the multivalent effect observed can be attributed exclusively to aggregation effects, as confirmed by the aggregation observed at the end of the ITC experiments (Fig. 7A). For the RSL lectin, the authors proposed a chelate binding between fucofullerenes and this lectin is most likely responsible for the binding enhancement (Fig. 7B). However, it is foreseeable that only a small amount of the sugar epitopes is participating at the same time, probably owing to steric hindrance around the fucofullerene derivatives after binding two or more lectins.

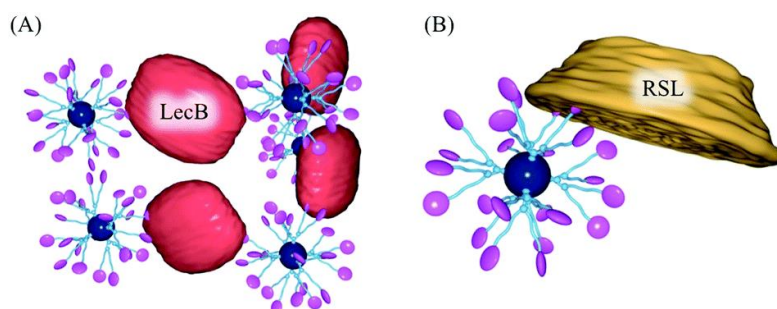


**Figure 7.** Schematic representation of the clustering resulting from the association of fucofullerene with LecB (A) and the simultaneous binding of two fucose units of fucofullerene to RSL (B). Image reproduced with permission from Royal Society of Chemistry.<sup>69</sup>

It is important to highlight that compound **24**, bearing 24 fucose units on the fullerene surface is one of the most potent ligands for both LecB and RSL lectins reported to date, showing the potential of glycofullerenes in anti-adhesive therapeutic applications.<sup>70-72</sup>

#### 2.4. Glycofullerenes as anticancer agents.

Recently, Serda *et al.*<sup>73</sup> have employed glycofullerenes as non-receptor tyrosine kinase inhibitors involved in pancreatic cancer. The glycofullerenes, decorated with D-glucosamine motifs bearing the free anomeric OH were conjugated via the C-2 amine to the central scaffold (Figure 8) and tested as potential inhibitors of non-receptor tyrosine kinases including the ABL1, BRK, BTK and Src family kinases (CSK, Fyn A, Lck, Lyn B and Src). Compound **25** showed a higher inhibitory activity profile than **26** for Src family kinases, as well as ABL1, BRK, and BTK kinases. This glyconanomaterial **25** presented the lowest value of the IC<sub>50</sub> parameter for Fyn A and BTK proteins and being able to selectively modulate the activity of both enzymes. This selectivity was owing to the formation of a protein corona around derivative **25**, confirmed by SDS-PAGE electrophoresis studies. Interestingly, both **25** and **26** appeared to be non-toxic for the pancreatic cancer cell cycle (tested in two human pancreatic cancer cell lines: PANC-1 and AsPC-1). However, the molecules induced autophagy and

disrupted redox balance, triggering the upregulation of repair systems and influencing the changing of Fyn and BTK protein levels in both pancreatic cancer cell lines.

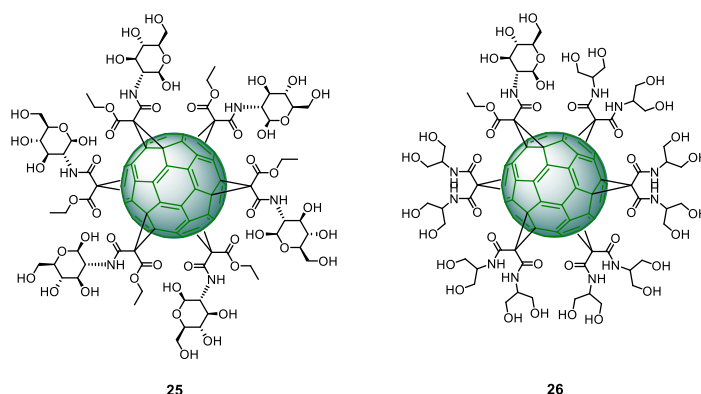


**Figure 8.** Structures of glycofullerenes **25-26**

Previously, the same authors carried out internalization studies of  $C_{60}(\text{GlcNAc})_6$  **25** in pancreatic stellate cells (PSCs) by co-localization studies,<sup>74</sup> which are involved with the establishment of dense stroma regions in cases of advanced pancreatic adenocarcinoma. As depicted in Figure 9, compound **25** was predominantly accumulated in the nucleus of PSCs and displayed strong photodynamic cytotoxic behavior, when illuminated with blue and green light.

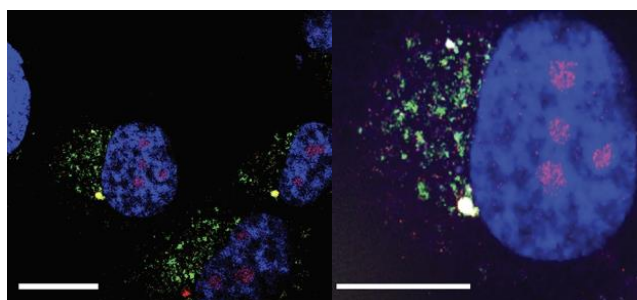


**Figure 9.** Confocal micrograph depicting pancreatic stellate cells blue regions and magenta represents antibody-glycofullerene **25** conjugate. Reproduced with permission from Future Medicine.<sup>74</sup>

These results represent the first example of [60]fullerene glycomaterials as selective non-receptor tyrosine kinases inhibitors, opening a new avenue for this kind of nanomaterials in the development of pancreatic cancer nanotherapeutics, as well as photodynamic therapy agents.

### 3. Glyco-carbon nanotubes (glycoCNTs).

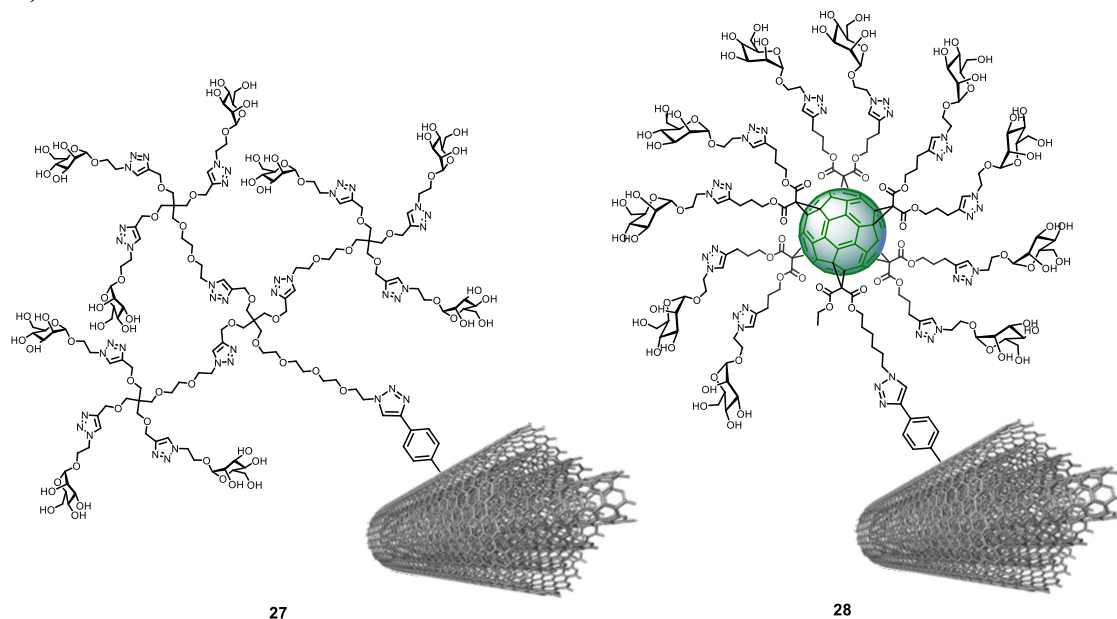
In addition to [60]fullerenes, other carbon nanostructures have also been developed for applications in the biological and medical fields.<sup>75-79</sup> These carbon-based nanomaterials, carbon nanotubes (CNTs), namely single and multi-walled carbon nanotubes (SWCNTs/MWCNTs), have attracted significant interest mostly due to their attractive electrical, physical, mechanical and chemical properties. To that end, different strategies for their surface functionalization have been developed<sup>80-83</sup> for different potential biological applications.<sup>84</sup> Although, in recent years, CNT-based glycoconjugates<sup>77, 85-90</sup> have received less

attention compared to [60]fullerene derivatives, CNT-based materials remain an unconventional and biocompatible platform that can help us study the multivalent effect in sugar-protein recognition processes. Here, we discuss the synthesis and biological applications of the most recent examples of CNT-based glycoconjugates.

### 3.1. GlycoCNTs as antiviral agents.

One of the most representative examples of nanocarbon-based glycoconjugates as multivalent inhibitors of viral infection, came from the group of Martin and co-workers,<sup>91</sup> where multivalent glycoconjugates **27-30** were described (Figure 10A). CNTs were chosen as a platform for glycan presentation because these multivalent nanosized glycoconjugates could mimic the shape or surface of EBOV, since the elongated shape of CNTs resembles the filamentous structure of this virus (Figure 10B). Glycoconjugates **27-30** were prepared starting by the chemical functionalization of the surface of the CNTs whereby alkyne groups were introduced, followed by a one-pot deprotection/CuAAC click reaction with the corresponding azide-substituted glycodendron or glycofullerene. In this way, it was possible to access materials that allowed the team to study the biological effect of both glycodendrons and glycofullerenes presentation systems.

A)



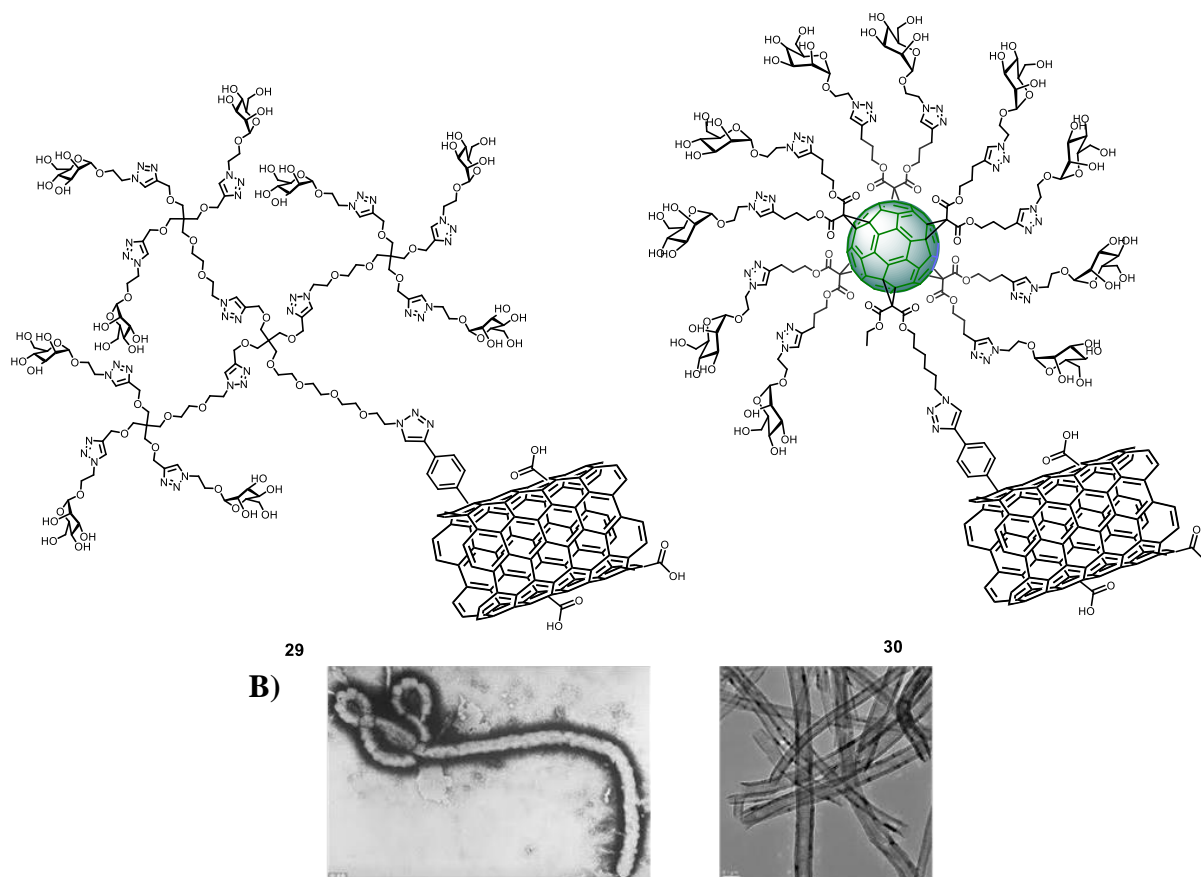


**Figure 10.** Structures of (A) glyconanomaterials **27-30** and (B) representation of filamentous structure of EBOV (left) and SWCNTs (right).

Characterization of these hybrid materials can be challenging, techniques such as DLS, thermogravimetric analysis (TGA), Raman spectroscopy, Fourier transform infrared spectroscopy (FTIR), X-ray photoelectron spectroscopy (XPS) and transmission electron microscopy (TEM) were all applied to provide insights into the physicochemical properties of the materials. Moreover, the antiviral activity of the nanoglycoconjugates decorated with mannose **27-30** was evaluated using pseudotyped viral particles which present EBOV glycoproteins on their surface in a similar way as described previously in section 2.1. It was found that the number of multivalent ligands was as important as the size and morphology of the scaffold used for their presentation. In particular, glycoconjugates based on 3D MWCNTs **28** resulted to be potent inhibitors of EBOV infection (Figure 11), with no appreciable cytotoxic effects. These CNFs can be considered novel efficient multivalent platforms which tunable size and high biostability properties make of them very appealing materials for the development of antivirals and other biomedical applications.

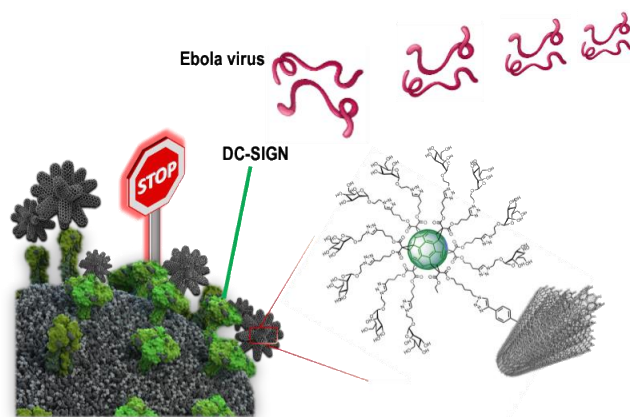


**Figure 11.** 3D MWCNTs glycoconjugates such as **28** as potent inhibitors of EBOV infection.

### 3.2. GlycoCNTs as anti-bacterial agents.

Recently, CNTs-based glycoconjugates where the scaffolds are assembled via non-covalent<sup>92, 93</sup> and covalent<sup>94</sup> bonds have been reported for anti-bacterial purposes. Khiar *et al.*<sup>92</sup> have developed a mannose-based polymerized glyconanorings capable of self-assembly on the surface of SWCNT with a non-covalent supramolecular fashion resulting in an abacus-like geometry after ultraviolet irradiation.

The water stable 1D-mannose-coated SWCNT **31** was characterized using conventional techniques used in material sciences such as NIR, TEM, AFM, DLS and Raman spectroscopy. First, the ability of **31** to specifically interact with Concanavalin A (ConA) lectin by the so-called enzyme-linked lectin assay (ELLA) was determined. This study showed a significant cluster glycoside effect with 2340-fold enhanced relative binding potency in sugar molar basis, with respect to the monovalent methyl  $\alpha$ -D-mannopyranoside control. Importantly, this finding was validated *in vitro* using an agglutination assay of the enterobacteria *E. coli* type 1 fimbriae (Figure 12A).<sup>92</sup>

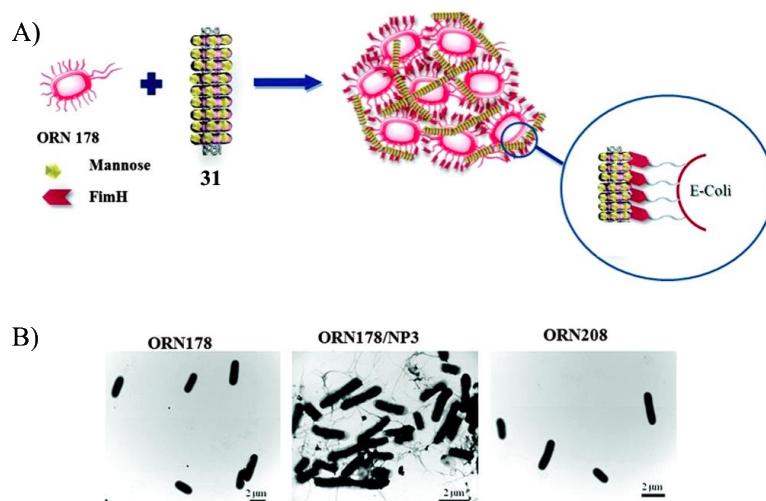


**Figure 12.** Schematic representation of the Fim H adhesin promoted specific interaction of *E. coli* with **31** (A) and TEM images of *E. coli* strains ORN178 and ORN208 alone, and ORN with **31** (B). Reproduced with permission from Royal Society of Chemistry.<sup>92</sup>

For this purpose, two different *E. coli* strains with and without the mannose receptor FimH were used, namely ORN178 and ORN208, respectively. The manno-CNT **31** showed efficient and selective regulation of the agglutination and proliferation of FimH-presenting *E. coli* type 1 fimbriae strain, observing a fireball-like cluster by thousands of bacteria as shown by high resolution TEM (Figure 12B). As expected, in the case of the FimH-devoid strain, inhibition of bacterial growth was not observed. More recently, the Khier group carried out the same study with glyco-CNTs where mannose and lactose residues were covalently attached to SWCNT.<sup>94</sup> In a similar way, the mannose-coated SWCNTs were able to agglutinate and inhibit in an efficient and selective manner the bacterial growth of *E. coli*, while the corresponding lactose-coated 1D-carbon nanotubes showed no formation of bacterial aggregates as expected since lactose is not a ligand for FimH. These findings highlight the potential of sugar-coated 1D-SWCNT as novel and effective antiadhesive drugs for the modulation of bacterial pathogenesis.

### 3.3. GlycoCNTs as anticancer agents.

Sugar-coated CNTs have also found applications as anticancer agents where the functionalization of MWCNT with the nonimmunogenic, biocompatible, biodegradable and noninflammatory hyaluronic acid (HA) was exploited.<sup>95,96</sup> The system, takes advantage of the overexpression of the HA-binding receptors e.g. cluster determinant 44 (CD44) on the surface of malignant cells. Therefore, HA-functionalized smart MWCNTs have been employed as anticancer drug nanocarriers to encapsulate doxorubicin (DOX) for targeted delivery to cancer cells.<sup>97</sup>

In 2018, Richichi *et al.*<sup>98</sup> reported the functionalization of MWCNT with GM3-lactone mimetic as an inhibitor of melanoma-associated metastatic events (Figure 13). For this purpose, the group investigated the effect of this nanosized glycoconjugate **32** on the metastatic-related events of A375 human melanoma cells, where they monitored cellular adhesion, migration and invasiveness properties. The *in vitro* results showed no toxicity for compound **32** and a great interference effect with A375 cell adhesion properties. Moreover, induction of strong inhibition on the migration and invasiveness of the melanoma cells was observed. These results taken together hold great potential for future applications of glyco-MWCNT against melanoma.

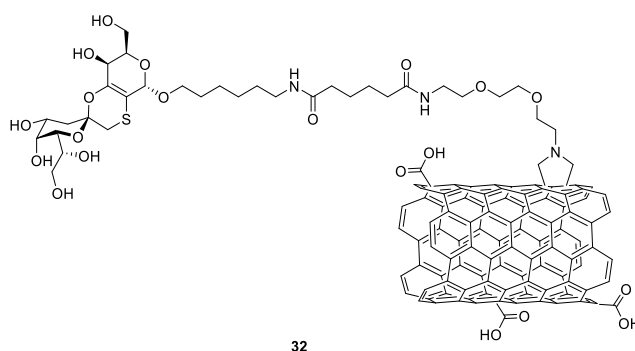


**Figure 13.** Structure of glyconanomaterial **32**.

## 4. Glycographenes.

Pristine graphene and its derivatives such as graphene oxide (GO)<sup>99</sup> and reduced graphene oxide (rGO)<sup>100</sup> similarly to CNTs have attracted wide scientific interest thanks to the high chemical stability, electrical conductivity and photoelectric properties. These, together with the



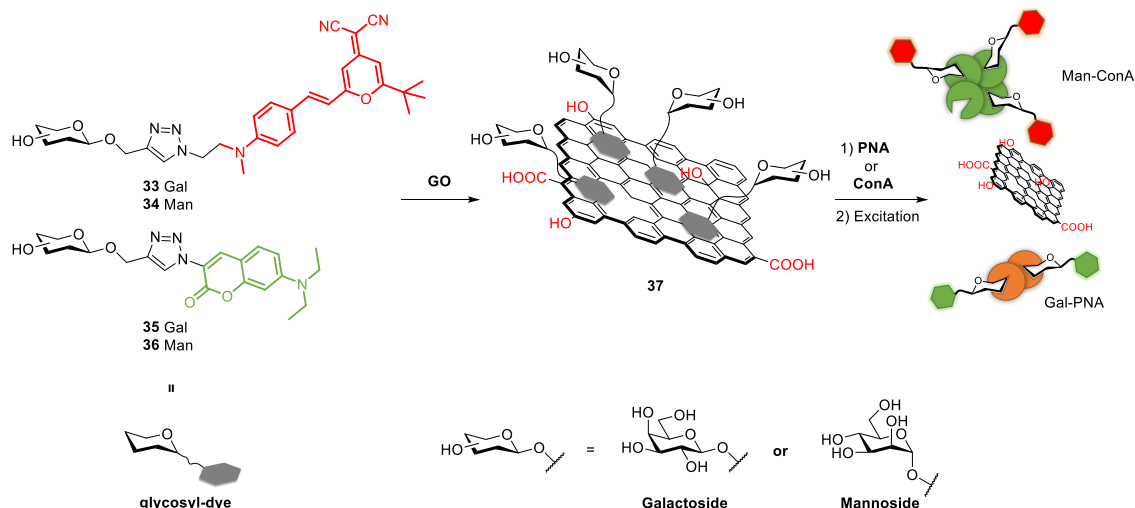
high biological tolerance exhibited by graphene derivatives have given rise to a plethora of applications as functional nanomaterials,<sup>101</sup> in nanomedicine,<sup>102</sup> microelectronics<sup>103</sup> and in the development of wearable devices<sup>104</sup> among others.

The glycan functionalization of graphene platforms either via covalent binding or non-covalent interactions has been adopted as a key strategy to increase the water solubility, colloidal stability and biocompatibility of these carbon-based nanomaterials. In most cases, the decoration of GO and rGO with glycoconjugates is achieved via  $\pi$ - $\pi$  staking interactions between the graphene scaffold and a glycosidic derivative functionalized with an aromatic moiety. However, some studies have also explored novel structures where single sugars<sup>105</sup> or polysaccharides<sup>106, 107</sup> can be covalently bound to either pristine graphene or rGO. In this section, we will highlight the most recent advances on the synthesis and applications of glyco-functionalized GO and rGO as biosensors and as antimicrobial and anti-cancer agents.

#### 4.1. Glycographene derivatives for biosensing applications.

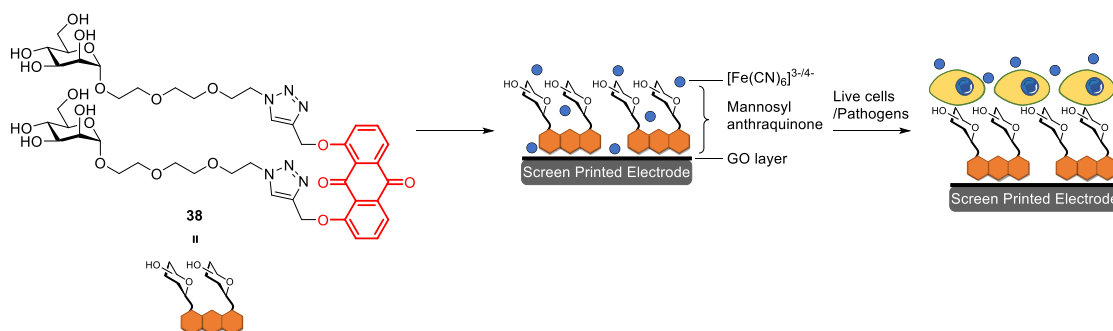
Glycan-decorated graphene probes were developed to exploit the strong and specific multivalent interaction between carbohydrates and their corresponding lectin receptors and used to detect lectins and lectin-expressing cells both *in vitro* and in complex matrixes.<sup>108</sup> For instance, the conjugation of glycosides to aromatic dyes led to the development of fluorescent glycoreporters adsorbed on the surface of graphene derivatives via  $\pi$ - $\pi$  staking interaction. This strategy has been exploited for improving the water solubility and reducing the toxicity of some organic dyes applied in imaging and sensing studies.<sup>109</sup> Glycographene derivatives have been evaluated most commonly in sugar/lectin models involving the use of glucose or mannose/ConA<sup>108</sup> and galactose/peanut agglutinin (PNA) interaction pairs.<sup>110</sup> These models served as preliminary *in vitro* studies to evaluate the efficiency and specificity of graphene glyconanocomposite prior to the study of more complex targets such as mannose receptors expressed on the surface of macrophages and dendritic cells, FimH protein expressed on the surface of *E. coli* and galactose-binding asialoglycoproteins expressed on the surface of hepatocytes, among others.<sup>111-113</sup>

A major contribution to the field of graphene glycoprobes has come from He and co-workers,<sup>114</sup> which recently developed a fluorescent probe for the simultaneous detection of galactose and mannose binding proteins. Galactose and mannose derivatives were conjugated to either dicyanomethylene ( $\lambda_{\text{ex}} = 460$  nm,  $\lambda_{\text{em(max)}} = 620$  nm) to furnish glycoconjugates **33** and **34**, respectively, or to aminocoumarin ( $\lambda_{\text{ex}} = 420$  nm,  $\lambda_{\text{em(max)}} = 500$  nm) to give galactose and mannose derivatives **35** and **36**, respectively. These sugar-dyes that can be simultaneously excited at 430 nm resulting in the emission of two distinct signals. The probes were grafted onto the GO platform which quenched the fluorescence of the dyes likely via Förster resonance energy transfer (FRET) as proposed by the authors, due to the GO's broad adsorption band. Interaction between the protein receptor and the GO-glycan complex results in the dissociation of the protein/glycoside-dye complex from the GO structure, restoring the fluorescent properties of the dyes (Scheme 1). The system allowed for the orthogonal identification of mannoside and galactoside receptors with a LOD of 37 and 44 nM for ConA and PNA, respectively.



**Scheme 1.** Structure of galactose- and mannose-dye conjugates **33-36** used for the complexation with GO to form **37** then tested with ConA, PNA or a combination of both to detect with a single excitation the simultaneous emission of the dissociated glycosyl-dyes.

Xie *et al.* have developed a graphene electro-sensors for live cell sensing applications, in which glycan-probes adsorbed onto GO allowed for the selective detection of live cells and pathogens expressing mannose-binding proteins.<sup>112</sup> Azide-functionalized mannosides were clicked with an anthraquinone moiety via CuAAC ligation to give **38** which was then grafted onto a GO-coated electrode. A diffusion-to-surface redox process employing  $[\text{Fe}(\text{CN})_6]^{3-/4-}$  was used to monitor the interaction between a mannose binding protein such as ConA and live cells expressing mannose-specific lectins *e.g.* tumour associated M2 macrophages and *E. coli* (Scheme 2). The mannose-receptor binding event created a shield that hampers the diffusion of Fe to the electrode surface with great specificity and linearity over an increasing concentration of ConA. The sensor was able to specifically recognize *E. coli* and M2 macrophages cells that express mannose-binding in complex matrices with a good linear response over a wide concentration range.



**Scheme 2.** Structure of mannosyl anthraquinone **38** and self assembled complex on GO-cated electrode. After the interaction with mannose-binding cells and pathogens the diffusion to the surface of the redox probe  $[\text{Fe}(\text{CN})_6]^{3-/4-}$  changes with linear concentration-dependence of the mannose-binding species.

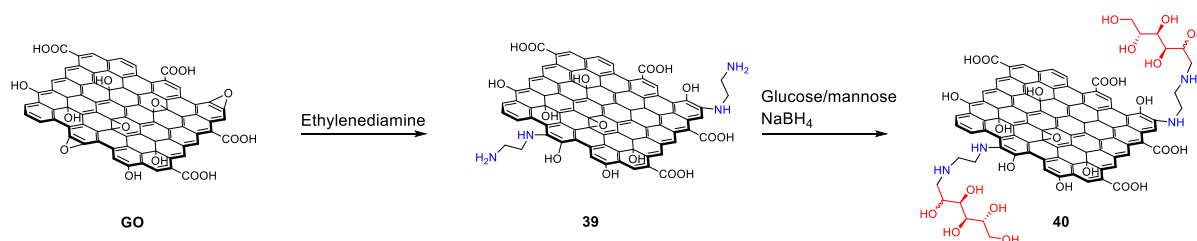
These exciting results obtained from glycan-functionalized graphene and its derivatives suggest these materials are promising targets for further development as biosensors. Novel

fluorescent or electrochemical probes with very low LOD can find applications in the screening of complex matrices for the accurate and early detection of cancers and pathogenic infections.

#### 4.2. Glycographene derivatives for antibacterial applications.

Due to the challenge posed by the emergence antibiotic-resistant microorganisms,<sup>115, 116</sup> the inert antibacterial properties exhibited by graphene and its derivatives, combined with low mammalian cytotoxicity, have prompted the investigation of novel graphene-based antibacterial agents.<sup>117</sup> Most graphite-based materials developed as antimicrobial agents owe their bioactivity to the combined effect of oxidative stress via the formation of superoxide radical anions ( $O_2^{\cdot-}$ ) and the destruction of the membrane integrity via graphene insertion and phospholipid extraction.<sup>118</sup>

The functionalization of graphene derivatives with different glycosides can be exploited for the enhancement of the antibacterial effect, and to gain specificity toward different bacterial strains which are known to bind to specific glycans as the first step on the bacterial infection process.<sup>119</sup> Recently, Chegeni *et al.* demonstrated how the mannose and glucose functionalization of GO resulted in enhanced antibacterial activity against two gram-negative bacteria, *K. pneumoniae* and *E. Coli* and two gram-positive bacteria, *B. cereus* and *S. aureus*.<sup>120</sup> Functionalization of GO with ethylenediamine gave intermediate **39** which was then decorated with unprotected sugars via reductive amination between the aldehyde function of the corresponding monosaccharide and the amino function of **39** furnishing glyco-derivative **40** (Scheme 3). Antimicrobial studies showed enhanced antibacterial activity against all the bacteria species for the glycan-functionalized materials with respect to the non-functionalized ones, likely due to membrane destruction and oxidative stress.



**Scheme 3.** Synthesis of glyco-GO derivative **40** via reductive amination of intermediate **39**.

Graphene-based materials possess unique IR-absorption properties that allow for the thermal conversion of near IR irradiation into heat. While laser irradiation in the near IR region is harmless for the majority of cells and tissues, graphene, rGO and thermally reduced GO (trGO) can absorb near IR radiation causing a localized increase of the temperature with consequent damage for the surrounding cells. Based on this mechanism, Seeberger and Haag reported the synthesis and application of a supramolecular mannose-functionalized trGO structure to be evaluated against *E. coli*.<sup>121</sup> trGO was thus functionalized with a short PEG linker exposing a terminal adamantyl moiety, which was used as an anchor point for the supramolecular assembly of heptamannosylated  $\beta$ -cyclodextrin **41** to give the glycosylated platform **42** (Figure 14). It was shown that the so formed trGO-cyclodextrin complex could efficiently wrap around *E. coli* via specific mannose-FimH lectin interactions favoring bacterial agglutination.

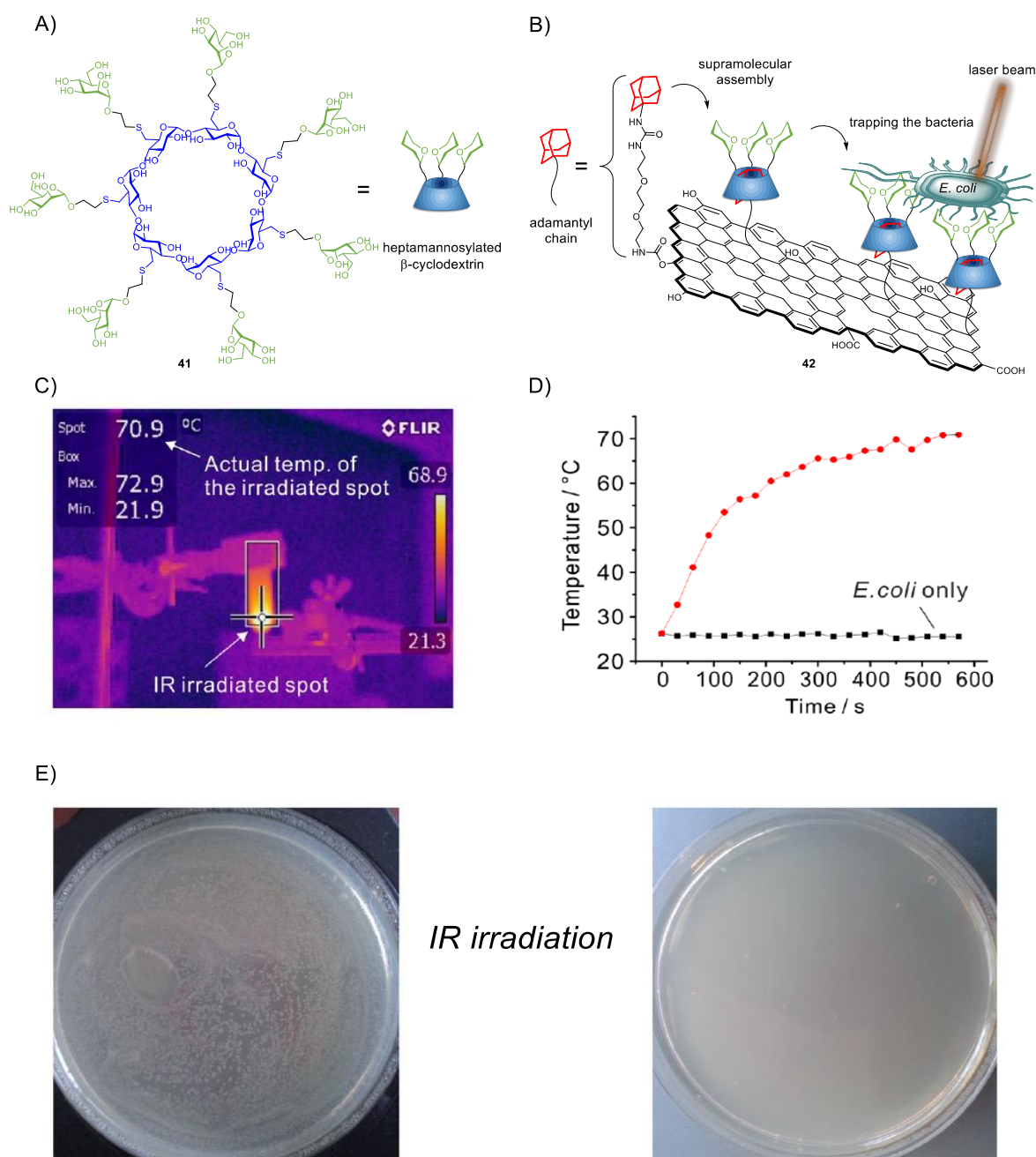


**Figure 14.** Structure of heptamannosylated  $\beta$ -cyclodextrin **41** (A), supramolecular assembly of cyclodextrin on adamantyl-functionalized trGO (**42**) and subsequent *E. coli* trapping and photothermal destruction (B), Thermal image of an *E. coli* sample incubated with **42** after 10 minutes of NIR laser irradiation ( $0.5 \text{ W/cm}^2$ ) (C), temperature evolution profiles of the *E. coli* samples with (red) and without (black) **42**, respectively (D), images of *E. coli* bacterial colonies treated with **42** without and with treatment of NIR irradiation (E). Reproduced with permission from American Chemical Society.<sup>121</sup>

The strong IR adsorption of trGO was then exploited for the photothermal killing of *E. coli*. After irradiation at 785 nm for 10 minutes >99 % of bacteria were efficiently killed upon a temperature increase to *ca.*  $70 \text{ }^\circ\text{C}$ . As negative control, non-irradiated bacteria could still form

large bacterial colonies after incubation with **42**. The strategy showed great specificity and on-demand bacteriostatic properties that could find further applications to help fight the antibiotic-resistant bacteria.

Graphene derivatives can interact with positively charged polysaccharides such as chitosan to form new composites materials with distinct physicochemical properties. Recent studies highlighted how the complexation of GO and rGO with chitosan strongly improve mammalian biocompatibility of graphene derivatives boosting at the same time the antibacterial properties of chitosan.<sup>122</sup> The positively charge chitosan interacts causing the rupture of negatively charged bacteria cells which makes of chitosan-based materials promising candidates for biomedical applications.<sup>123</sup> In a recent example, Rostami *et al.* reported the preparation of a sharkskin mimicked GO/chitosan membrane. This novel material significantly reduced *E. coli* and *S. aureus* biofilm formation preserving high biocompatibility with no toxic effect on mammalian cells.<sup>124</sup> In a recent study Rahnamaee *et al.* exploited the combined antibacterial properties of chitosan with the bacterial membrane rupture and oxidative stress provided by rGO to coat titania nanotubes with rGO/chitosan to create a ternary nanocomposite. The chitosan coating promoted controlled drug release of vancomycin loaded titania nanotube promoting at the same time bone cell viability with the intrinsic chitosan antibacterial properties. Moreover, rGO decreased the adhesion of bacteria on the surface providing together with chitosan a synergistic effect for long term antibacterial properties.<sup>125</sup>

### **4.3. Glycographenes derivatives for anticancer applications**

GO-based materials have also attracted significant attention as nanocarriers for targeted and controlled delivery of anticancer drugs and localized photothermal treatment of tumours thanks to their low mammalian cell toxicity. For example lactose<sup>126</sup> and galactose<sup>127, 128</sup> functionalization of GO was exploited for the selective delivery of glycographene derivatives to hepatoma cells. These cells overexpress an asialoglycoprotein lectin receptor that binds to non-sialylated glycans for the removal of asialylated proteins (*e.g.* old immunoglobulins) from circulation. On the other hand, functionalization of GO and rGO with mannose derivatives produced probes used to target mannose receptors overexpressed in macrophages and dendritic cells for drug delivery applications.<sup>129, 130</sup>

The tremendous potential of photothermal therapy in cancer treatment relies on the very low toxicity of the drug-loaded probes in the absence of NIR radiation. NIR can be applied with great topological specificity using a laser which triggers the cargo release and thermal cellular destruction.<sup>120-131</sup> Nonetheless, in order to improve the biocompatibility of rGO, several research groups have found different ways to avoid the use of the toxic hydrazine hydrate as reducing agent for GO reduction, by replacing it with fucoidan<sup>132</sup> or L-ascorbic acid,<sup>131</sup> among others. Many nanoparticle-based drug delivery systems take advantage of the so-called enhanced permeability and retention effect (EPR) for the passive accumulation inside the leaky tumour vasculature.<sup>133</sup> However, in order to improve the active specific targeting of cancer cells and tissues, the functionalization of the probes with glycopolymers such as HA was used to enhance the nanomaterial cellular internalization in malignant cells that overexpress HA binding receptor CD44. In a recent approach developed by Liang *et al.*, magnetic Fe<sub>3</sub>O<sub>4</sub>-GO was coated with HA previously functionalized with  $\beta$ -cyclodextrin which was able to bind the GO layer via non covalent interactions, DOX was subsequently loaded and trapped inside the lipophilic cyclodextrin hole.<sup>134</sup> The system allowed for the nanomaterial

cellular internalization via CD44-mediated endocytosis and the release of the DOX cargo was amplified by the photothermal temperature increase promoted by NIR irradiation.

A different approach was proposed by Zhou and Huo using a temperature and redox sensitive HA-GO system.<sup>135</sup> In this composite, HA was covalently attached to GO through redox sensitive disulphide linker (cystamine) followed by DOX loading (Figure 15). HA was initially functionalized via amide bond formation to give disulphide derivative **43**, which could be covalently anchored HA on the GO surface via amidation between the free amines on the linker and the GO acidic residues. DOX was finally loaded on the GO surface via lipophilic interactions furnishing composite **44**. The covalently attached HA granted the nanomaterial further chemical and colloidal stability increasing the circulation time in physiological conditions.

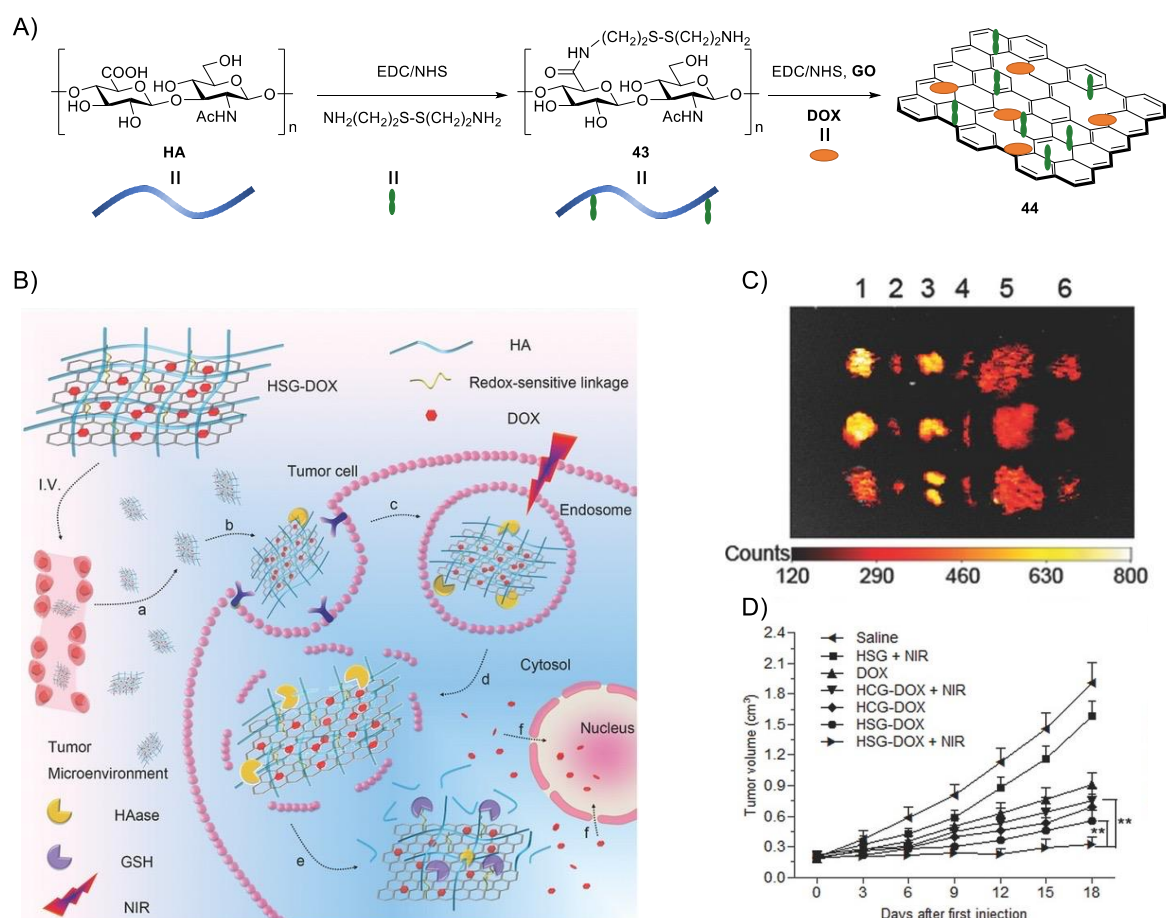


**Figure 15.** Functionalization of HA to give redox sensitive glycopolymer **43** then attached onto GO surface via EDC/NHS promoted amidation and functionalization with DOX to give nanocomposite **44** (A), NIR irradiation-controlled endo/lysosomal escape for tumor cytoplasm-selective delivery and GSH-triggered rapid release of DOX in cytoplasm, which led to enhanced accumulation of DOX into nuclei for enhanced cancer treatment: a) accumulation of HSG-DOX within the tumor site through passive and active targeting effects; b,c) receptor-mediated cellular internalization; d) HAase-mediated HA degradation in endosomes and NIR-mediated endo/lysosomal escape; e) GSH triggered HA detachment and rapid DOX release in cytoplasm; f) accumulation of released DOX into nucleus for DNA damage-mediated apoptosis and cytotoxicity (B), Ex vivo Cy7 fluorescence imaging of the tumor and normal tissues of the MDA-MB-231 tumor-bearing nude mice after mice were euthanized at 36 h postinjection. 1, 2, 3, 4, 5, 6 (C), and Tumor volume (cm<sup>3</sup>) vs Days after first injection (D).

tumor; 2, heart; 3, kidney; 4, spleen; 5, liver; and 6, lung (C), and Tumor growth curves after intravenous injection of different formulations at a DOX dose of 5 mg kg<sup>-1</sup>. \*\*P < 0.01 (D). Reproduced in part with permission from Wiley.<sup>135</sup>

The team showed the nanoparticle accumulated in tumour cells by the combined EPR effect and the interaction between HA and the CD44 receptor. The system was then internalized inside tumour cells in endo/lysosomes where hyaluronidase enzyme digested HA in small fragments. After NIR irradiation at 808 nm, the local heat generated by the photothermal effect (up to 72 °C measured *in vitro*) destroyed the endo/lysosomal membrane followed by cytoplasmic glutathione-promoted reduction of the disulfide bond in the cystamine linker. This cascade of events led to the cleavage of residual HA promoting DOX release into the cytoplasm. This system allowed for improved and controlled DOX release and cytotoxicity in both *in vitro* and *in vivo* in BALB/c mice bearing MDA-MB-231 xenograft models and noticeable tumour growth suppression was observed.

## 5. Conclusions and Future Challenges

In the search for new pathways to study disease-relevant carbohydrate-mediated processes, such as viral infection, cancer or antibacterial inhibition, the scientific community has focused in the last few years on the development of multifunctional probes to allow the study of carbohydrate-protein interactions and their multivalency. Within this context, carbon nanosized structures appear to be ideal candidates for the generation of probes that can present multiple copies of a glycan on interest with tunable characteristics. Fullerenes, nanotubes and graphene and their corresponding derivatives should be considered as very promising and biocompatible scaffolds for the globular multivalent presentation of sugars. Since not only multivalency, but also the size and shape of the carbon nanoplatform employed appear to be very important for the successful interaction of glycans with their corresponding cellular receptors, it becomes clear the careful choice of the carbon nanoform as scaffold is very important when designing multivalent nanosized glycoconjugates. For example, glyco-carbon nanotubes or nanohorns can mimic the shape or surface of specific viruses, such as Ebola virus or HIV. The rapid growing field of carbon-based nanomaterials has led to the development of a great range of novel carbon nanoforms, such as carbon nanoions, peapods, carbon nanotori, carbon nanobuds and more recently 2D graphene quantum dots (GQDs) and carbon quantum dots (CQDs) and 3D carbon dots (CDots),<sup>136-141</sup> which could also be used as potential scaffolds for the multivalent presentation of carbohydrates. The control of the carbohydrate functionalization and distribution on a given nanostructures and their structural characterization still represent a future scientific challenge. On the other hand, taking into account the enormous variety of potential carbohydrates, both in terms of their structure (e.g., monosaccharides, disaccharides, polysaccharides, etc.) and surface presentation (e.g., defined dendrimers, degree of surface functionalization), a wide range of combinations of multivalent nanosized glycoconjugates can be prepared. In this context, methods to efficiently select the correct ligand(s) and adequate surface presentation on different scaffolds will eventually furnish a variety of lead hybrid molecules with high specificity and efficiency for bespoke applications. Considering the avant-garde developments in carbon nanoform chemistry, glycobiology and nanotechnology, a great progress is expected in the near future from their synergistic blend.

## Conflict of interest

There are no conflicts to declare.

## Acknowledgments

MCG and MG would like to thank the European Research Council (ERC- COG: 648239) for funding and J. R.-S. thanks MSCA fellowship (project 843720-BioNanoProbes). This publication has risen from discussion at COST Action GLYCONanoPROBES (CA18132), supported by COST (European Cooperation in Science and Technology).

Manuscript in honor of Prof. Jesus Jimenez Barbero's 60<sup>th</sup> birthday – Felicidades.

## References

1. Zhang, X. T.; Liu, G. J.; Ning, Z. W.; Xing, G. W., Boronic acid-based chemical sensors for saccharides. *Carbohydr. Res.* **2017**, *452*, 129-148.
2. Varki, A., Biological roles of glycans. *Glycobiology* **2017**, *27* (1), 3-49.
3. Kaltner, H.; Abad-Rodriguez, J.; Corfield, A. P.; Kopitz, J.; Gabius, H. J., The sugar code: letters and vocabulary, writers, editors and readers and biosignificance of functional glycan-lectin pairing. *Biochem J* **2019**, *476*, 2623-2655.
4. Lundquist, J. J.; Toone, E. J., The cluster glycoside effect. *Chem Rev* **2002**, *102* (2), 555-578.
5. Lee, R. T.; Lee, Y. C., Affinity enhancement by multivalent lectin-carbohydrate interaction. *Glycoconjugate J* **2000**, *17* (7-9), 543-551.
6. Muller, C.; Despras, G.; Lindhorst, T. K., Organizing multivalency in carbohydrate recognition. *Chem Soc Rev* **2016**, *45* (11), 3275-3302.
7. Jayaraman, N., Multivalent ligand presentation as a central concept to study intricate carbohydrate-protein interactions. *Chem Soc Rev* **2009**, *38* (12), 3463-3483.
8. Richards, S.-J.; Otten, L.; Gibson, M. I., Glycosylated gold nanoparticle libraries for label-free multiplexed lectin biosensing. *J. Mater. Chem. B* **2016**, *4* (18), 3046-3053.
9. Khan, H.; Mirzaei, H. R.; Amiri, A.; Kupeli Akkol, E.; Ashhad Halimi, S. M.; Mirzaei, H., Glyco-nanoparticles: New drug delivery systems in cancer therapy. *Seminars in Cancer Biology* **2019**.
10. Zhang, X.; Huang, G.; Huang, H., The glyconanoparticle as carrier for drug delivery. *Drug Delivery* **2018**, *25* (1), 1840-1845.
11. Shengju, Z.; Piotr, T.; Lili, S.; Sen, H.; Hongguang, L., Sugar-Functionalized Fullerenes. *Current Organic Chemistry* **2016**, *20* (14), 1490-1501.
12. Castro, E.; Garcia, A. H.; Zavala, G.; Echegoyen, L., Fullerenes in biology and medicine. *J. Mater. Chem. B* **2017**, *5* (32), 6523-6535.
13. Illescas, B. M.; Rojo, J.; Delgado, R.; Martín, N., Multivalent Glycosylated Nanostructures To Inhibit Ebola Virus Infection. *Journal of the American Chemical Society* **2017**, *139* (17), 6018-6025.
14. Nierengarten, I.; Nierengarten, J.-F., Fullerene Sugar Balls: A New Class of Biologically Active Fullerene Derivatives. *Chemistry – An Asian Journal* **2014**, *9* (6), 1436-1444.
15. Muñoz, A.; Illescas, B. M.; Luczkowiak, J.; Lasala, F.; Ribeiro-Viana, R.; Rojo, J.; Delgado, R.; Martín, N., Antiviral activity of self-assembled glycodendro[60]fullerene monoadducts. *J. Mater. Chem. B* **2017**, *5* (32), 6566-6571.
16. Nierengarten, J.-F.; Iehl, J.; Oerthel, V.; Holler, M.; Illescas, B. M.; Muñoz, A.; Martín, N.; Rojo, J.; Sánchez-Navarro, M.; Cecioni, S.; Vidal, S.; Buffet, K.; Durka, M.; Vincent, S. P., Fullerene sugar balls. *Chemical Communications* **2010**, *46* (22), 3860-3862.
17. Sánchez-Navarro, M.; Muñoz, A.; Illescas, B. M.; Rojo, J.; Martín, N., [60]Fullerene as Multivalent Scaffold: Efficient Molecular Recognition of Globular Glycofullerenes by Concanavalin A. *Chemistry – A European Journal* **2011**, *17* (3), 766-769.



18. Luczkowiak, J.; Muñoz, A.; Sánchez-Navarro, M.; Ribeiro-Viana, R.; Ginieis, A.; Illescas, B. M.; Martín, N.; Delgado, R.; Rojo, J., Glycofullerenes Inhibit Viral Infection. *Biomacromolecules* **2013**, *14* (2), 431-437.
19. Alvarez, C. P.; Lasala, F.; Carrillo, J.; Muñiz, O.; Corbí, A. L.; Delgado, R., C-Type Lectins DC-SIGN and L-SIGN Mediate Cellular Entry by Ebola Virus in *Journal of Virology* **2002**, *76* (13), 6841.
20. Lüdtke, A.; Ruibal, P.; Wozniak, D. M.; Pallasch, E.; Wurr, S.; Bockholt, S.; Gómez-Medina, S.; Qiu, X.; Kobinger, G. P.; Rodríguez, E.; Günther, S.; Krasemann, S.; Idoyaga, J.; Oestereich, L.; Muñoz-Fontela, C., Ebola virus infection kinetics in chimeric mice reveal a key role of T cells as barriers for virus dissemination. *Scientific Reports* **2017**, *7* (1), 43776.
21. Perera-Lecoin, M.; Meertens, L.; Carnec, X.; Amara, A., Flavivirus Entry Receptors: An Update. *Viruses* **2014**, *6* (1).
22. Hamel, R.; Dejarnac, O.; Wichit, S.; Ekchariyawat, P.; Neyret, A.; Luplertlop, N.; Perera-Lecoin, M.; Surasombatpattana, P.; Talignani, L.; Thomas, F.; Cao-Lormeau, V.-M.; Choumet, V.; Briant, L.; Desprès, P.; Amara, A.; Yssel, H.; Missé, D., Biology of Zika Virus Infection in Human Skin Cells. *Journal of Virology* **2015**, *89* (17), 8880.
23. Ramos-Soriano, J.; de la Fuente, M. C.; de la Cruz, N.; Figueiredo, R. C.; Rojo, J.; Reina, J. J., Straightforward synthesis of Man9, the relevant epitope of the high-mannose oligosaccharide. *Organic & Biomolecular Chemistry* **2017**, *15* (42), 8877-8882.
24. Muñoz, A.; Sigwalt, D.; Illescas, B. M.; Luczkowiak, J.; Rodríguez-Pérez, L.; Nierengarten, I.; Holler, M.; Remy, J.-S.; Buffet, K.; Vincent, S. P.; Rojo, J.; Delgado, R.; Nierengarten, J.-F.; Martín, N., Synthesis of giant globular multivalent glycofullerenes as potent inhibitors in a model of Ebola virus infection. *Nature Chemistry* **2016**, *8* (1), 50-57.
25. Engström, O.; Muñoz, A.; Illescas, B. M.; Martín, N.; Ribeiro-Viana, R.; Rojo, J.; Widmalm, G., Investigation of glycofullerene dynamics by NMR spectroscopy. *Organic & Biomolecular Chemistry* **2015**, *13* (32), 8750-8755.
26. Ramos-Soriano, J.; Reina, J. J.; Illescas, B. M.; de la Cruz, N.; Rodríguez-Pérez, L.; Lasala, F.; Rojo, J.; Delgado, R.; Martín, N., Synthesis of Highly Efficient Multivalent Disaccharide/[60]Fullerene Nanoballs for Emergent Viruses. *Journal of the American Chemical Society* **2019**, *141* (38), 15403-15412.
27. Ramos-Soriano, J.; Reina, J. J.; Pérez-Sánchez, A.; Illescas, B. M.; Rojo, J.; Martín, N., Cyclooctyne [60]fullerene hexakis adducts: a globular scaffold for copper-free click chemistry. *Chemical Communications* **2016**, *52* (69), 10544-10546.
28. Ramos-Soriano, J.; Reina, J. J.; Illescas, B. M.; Rojo, J.; Martín, N., Maleimide and Cyclooctyne-Based Hexakis-Adducts of Fullerene: Multivalent Scaffolds for Copper-Free Click Chemistry on Fullerenes. *The Journal of Organic Chemistry* **2018**, *83* (4), 1727-1736.
29. Wadood, A.; Ghufraan, M.; Khan, A.; Azam, S. S.; Jelani, M.; Uddin, R., Selective glycosidase inhibitors: A patent review (2012–present). *International Journal of Biological Macromolecules* **2018**, *111*, 82-91.
30. Dehoux-Baudoin, C.; Génisson, Y., C-Branched Imino Sugars: Synthesis and Biological Relevance. *European Journal of Organic Chemistry* **2019**, *2019* (30), 4765-4777.
31. Greimel, P.; Spreitz, J.; Stutz, A. E.; Wrodnigg, T. M., Iminosugars and Relatives as Antiviral and Potential Anti-infective Agents. *Current Topics in Medicinal Chemistry* **2003**, *3* (5), 513-523.
32. Rye, P. D.; Bovin, N. V.; Vlasova, E. V.; Walker, R. A., Monoclonal antibody LU-BCRU-G7 against a breast tumour-associated glycoprotein recognizes the disaccharide Gal $\beta$ 1-3GlcNAc. *Glycobiology* **1995**, *5* (4), 385-389.
33. Ashona, S.; Ndumiso, M.; Mahmoud, E. S. S., Anti-cancer Glycosidase Inhibitors from Natural Products: A Computational and Molecular Modelling Perspective. *Anti-Cancer Agents in Medicinal Chemistry* **2015**, *15* (8), 933-946.
34. Moscona, A., Neuraminidase Inhibitors for Influenza. *New England Journal of Medicine* **2005**, *353* (13), 1363-1373.

35. Rehana, D.; Mahendiran, D.; Kumar, R. S.; Rahiman, A. K., In vitro antioxidant and antidiabetic activities of zinc oxide nanoparticles synthesized using different plant extracts. *Bioprocess and Biosystems Engineering* **2017**, *40* (6), 943-957.
36. Balan, K.; Qing, W.; Wang, Y.; Liu, X.; Palvannan, T.; Wang, Y.; Ma, F.; Zhang, Y., Antidiabetic activity of silver nanoparticles from green synthesis using *Lonicera japonica* leaf extract. *RSC Advances* **2016**, *6* (46), 40162-40168.
37. Naik, M. Z.; Meena, S. N.; Ghadi, S. C.; Naik, M. M.; Salker, A. V., Evaluation of silver-doped indium oxide nanoparticles as in vitro  $\alpha$ -amylase and  $\alpha$ -glucosidase inhibitors. *Medicinal Chemistry Research* **2016**, *25* (3), 381-389.
38. Yuzwa, S. A.; Vocadlo, D. J., O-GlcNAc and neurodegeneration: biochemical mechanisms and potential roles in Alzheimer's disease and beyond. *Chem Soc Rev* **2014**, *43* (19), 6839-6858.
39. Wennekes, T.; van den Berg, R. J. B. H. N.; Boot, R. G.; van der Marel, G. A.; Overkleeft, H. S.; Aerts, J. M. F. G., Glycosphingolipids—Nature, Function, and Pharmacological Modulation. *Angewandte Chemie International Edition* **2009**, *48* (47), 8848-8869.
40. Wang, L.; Hu, C.; Shao, L., The antimicrobial activity of nanoparticles: present situation and prospects for the future. *Int J Nanomedicine* **2017**, *12*, 1227-1249.
41. Ahmed, K. B. A.; Raman, T.; Veerappan, A., Future prospects of antibacterial metal nanoparticles as enzyme inhibitor. *Materials Science and Engineering: C* **2016**, *68*, 939-947.
42. Decroocq, C.; Rodríguez-Lucena, D.; Russo, V.; Mena Barragán, T.; Ortiz Mellet, C.; Compain, P., The Multivalent Effect in Glycosidase Inhibition: Probing the Influence of Architectural Parameters with Cyclodextrin-based Iminosugar Click Clusters. *Chemistry – A European Journal* **2011**, *17* (49), 13825-13831.
43. Decroocq, C.; Rodríguez-Lucena, D.; Ikeda, K.; Asano, N.; Compain, P., Cyclodextrin-Based Iminosugar Click Clusters: The First Examples of Multivalent Pharmacological Chaperones for the Treatment of Lysosomal Storage Disorders. *ChemBioChem* **2012**, *13* (5), 661-664.
44. Decroocq, C.; Joosten, A.; Sergent, R.; Mena Barragán, T.; Ortiz Mellet, C.; Compain, P., The Multivalent Effect in Glycosidase Inhibition: Probing the Influence of Valency, Peripheral Ligand Structure, and Topology with Cyclodextrin-Based Iminosugar Click Clusters. *ChemBioChem* **2013**, *14* (15), 2038-2049.
45. Joosten, A.; Schneider, J. P.; Lepage, M. L.; Tarnus, C.; Bodlenner, A.; Compain, P., A Convergent Strategy for the Synthesis of Second-Generation Iminosugar Clusters Using “Clickable” Trivalent Dendrons. *European Journal of Organic Chemistry* **2014**, *2014* (9), 1866-1872.
46. Brissonnet, Y.; Ortiz Mellet, C.; Morandat, S.; Garcia Moreno, M. I.; Deniaud, D.; Matthews, S. E.; Vidal, S.; Šesták, S.; El Kirat, K.; Gouin, S. G., Topological Effects and Binding Modes Operating with Multivalent Iminosugar-Based Glycoclusters and Mannosidases. *Journal of the American Chemical Society* **2013**, *135* (49), 18427-18435.
47. Bonduelle, C.; Huang, J.; Mena-Barragán, T.; Ortiz Mellet, C.; Decroocq, C.; Etamé, E.; Heise, A.; Compain, P.; Lecommandoux, S., Iminosugar-based glycopolypeptides: glycosidase inhibition with bioinspired glycoprotein analogue micellar self-assemblies. *Chemical Communications* **2014**, *50* (25), 3350-3352.
48. Lepage, M. L.; Meli, A.; Bodlenner, A.; Tarnus, C.; De Riccardis, F.; Izzo, I.; Compain, P., Synthesis of the first examples of iminosugar clusters based on cyclopeptoid cores. *Beilstein J Org Chem* **2014**, *10*, 1406-1412.
49. Lepage, M. L.; Schneider, J. P.; Bodlenner, A.; Meli, A.; De Riccardis, F.; Schmitt, M.; Tarnus, C.; Nguyen-Huynh, N.-T.; Francois, Y.-N.; Leize-Wagner, E.; Birck, C.; Cousido-Siah, A.; Podjarny, A.; Izzo, I.; Compain, P., Iminosugar-Cyclopeptoid Conjugates Raise Multivalent Effect in Glycosidase Inhibition at Unprecedented High Levels. *Chemistry – A European Journal* **2016**, *22* (15), 5151-5155.
50. Brissonnet, Y.; Ladevèze, S.; Tezé, D.; Fabre, E.; Deniaud, D.; Daligault, F.; Tellier, C.; Šesták, S.; Remaud-Simeon, M.; Potocki-Veronese, G.; Gouin, S. G., Polymeric Iminosugars Improve the Activity of Carbohydrate-Processing Enzymes. *Bioconjugate Chemistry* **2015**, *26* (4), 766-772.

51. Siriwardena, A.; Khanal, M.; Barras, A.; Bande, O.; Mena-Barragán, T.; Mellet, C. O.; Garcia Fernández, J. M.; Boukherroub, R.; Szunerits, S., Unprecedented inhibition of glycosidase-catalyzed substrate hydrolysis by nanodiamond-grafted O-glycosides. *RSC Advances* **2015**, *5* (122), 100568-100578.
52. Compain, P.; Bodlenner, A., The Multivalent Effect in Glycosidase Inhibition: A New, Rapidly Emerging Topic in Glycoscience. *ChemBioChem* **2014**, *15* (9), 1239-1251.
53. Kanfar, N.; Bartolami, E.; Zelli, R.; Marra, A.; Winum, J.-Y.; Ulrich, S.; Dumy, P., Emerging trends in enzyme inhibition by multivalent nanoconstructs. *Organic & Biomolecular Chemistry* **2015**, *13* (39), 9894-9906.
54. Gouin, S. G., Multivalent Inhibitors for Carbohydrate-Processing Enzymes: Beyond the “Lock-and-Key” Concept. *Chemistry – A European Journal* **2014**, *20* (37), 11616-11628.
55. Nierengarten, J. F.; Schneider, J. P.; Trinh, T. M. N.; Joosten, A.; Holler, M.; Lepage, M. L.; Bodlenner, A.; Garcia-Moreno, M. I.; Mellet, C. O.; Compain, P., Giant Glycosidase Inhibitors: First- and Second-Generation Fullerodendrimers with a Dense Iminosugar Shell. *Chem-Eur J* **2018**, *24* (10), 2483-2492.
56. Trinh, T. M. N.; Holler, M.; Schneider, J. P.; Garcia-Moreno, M. I.; Fernandez, J. M. G.; Bodlenner, A.; Compain, P.; Mellet, C. O.; Nierengarten, J. F., Construction of giant glycosidase inhibitors from iminosugar-substituted fullerene macromonomers. *J. Mater. Chem. B* **2017**, *5* (32), 6546-6556.
57. Abellán Flos, M.; García Moreno, M. I.; Ortiz Mellet, C.; García Fernández, J. M.; Nierengarten, J.-F.; Vincent, S. P., Potent Glycosidase Inhibition with Heterovalent Fullerenes: Unveiling the Binding Modes Triggering Multivalent Inhibition. *Chemistry – A European Journal* **2016**, *22* (32), 11450-11460.
58. Compain, P.; Decroocq, C.; Iehl, J.; Holler, M.; Hazelard, D.; Mena Barragán, T.; Ortiz Mellet, C.; Nierengarten, J.-F., Glycosidase Inhibition with Fullerene Iminosugar Balls: A Dramatic Multivalent Effect. *Angewandte Chemie International Edition* **2010**, *49* (33), 5753-5756.
59. Mena-Barragán, T.; Narita, A.; Matias, D.; Tiscornia, G.; Nanba, E.; Ohno, K.; Suzuki, Y.; Higaki, K.; Garcia Fernández, J. M.; Ortiz Mellet, C., pH-Responsive Pharmacological Chaperones for Rescuing Mutant Glycosidases. *Angewandte Chemie International Edition* **2015**, *54* (40), 11696-11700.
60. Arroba, A. I.; Alcalde-Estevez, E.; García-Ramírez, M.; Cazzoni, D.; de la Villa, P.; Sánchez-Fernández, E. M.; Mellet, C. O.; García Fernández, J. M.; Hernández, C.; Simó, R.; Valverde, Á. M., Modulation of microglia polarization dynamics during diabetic retinopathy in db/db mice. *Biochimica et Biophysica Acta (BBA) - Molecular Basis of Disease* **2016**, *1862* (9), 1663-1674.
61. Sánchez-Fernández, E. M.; Gonçalves-Pereira, R.; Rísquez-Cuadro, R.; Plata, G. B.; Padrón, J. M.; García Fernández, J. M.; Ortiz Mellet, C., Influence of the configurational pattern of sp<sup>2</sup>-iminosugar pseudo N-, S-, O- and C-glycosides on their glycoside inhibitory and antitumor properties. *Carbohydr. Res.* **2016**, *429*, 113-122.
62. Fernández, E. M. S.; Navo, C. D.; Martínez-Sáez, N.; Gonçalves-Pereira, R.; Somovilla, V. J.; Avenoz, A.; Busto, J. H.; Bernardes, G. J. L.; Jiménez-Osés, G.; Corzana, F.; Fernández, J. M. G.; Mellet, C. O.; Peregrina, J. M., Tn Antigen Mimics Based on sp<sup>2</sup>-Iminosugars with Affinity for an anti-MUC1 Antibody. *Organic Letters* **2016**, *18* (15), 3890-3893.
63. García-Moreno, M. I.; de la Mata, M.; Sánchez-Fernández, E. M.; Benito, J. M.; Díaz-Quintana, A.; Fustero, S.; Nanba, E.; Higaki, K.; Sánchez-Alcázar, J. A.; García Fernández, J. M.; Ortiz Mellet, C., Fluorinated Chaperone-β-Cyclodextrin Formulations for β-Glucocerebrosidase Activity Enhancement in Neuronopathic Gaucher Disease. *Journal of Medicinal Chemistry* **2017**, *60* (5), 1829-1842.
64. Stauffert, F.; Bodlenner, A.; Nguyet Trinh, T. M.; García-Moreno, M. I.; Ortiz Mellet, C.; Nierengarten, J.-F.; Compain, P., Understanding multivalent effects in glycosidase inhibition using C-glycoside click clusters as molecular probes. *New Journal of Chemistry* **2016**, *40* (9), 7421-7430.

65. Videira, P. A.; Marcelo, F.; Grewal, R. K., Glycosyltransferase inhibitors: a promising strategy to pave a path from laboratory to therapy. In *Carbohydrate Chemistry: Chemical and Biological Approaches Volume 43*, The Royal Society of Chemistry: 2018; Vol. 43, pp 135-158.
66. Durka, M.; Buffet, K.; Iehl, J.; Holler, M.; Nierengarten, J.-F.; Vincent, S. P., The Inhibition of Liposaccharide Heptosyltransferase WaaC with Multivalent Glycosylated Fullerenes: A New Mode of Glycosyltransferase Inhibition. *Chemistry – A European Journal* **2012**, *18* (2), 641-651.
67. Tikad, A.; Fu, H.; Sevrain, C. M.; Laurent, S.; Nierengarten, J.-F.; Vincent, S. P., Mechanistic Insight into Heptosyltransferase Inhibition by using Kdo Multivalent Glycoclusters. *Chemistry – A European Journal* **2016**, *22* (37), 13147-13155.
68. Buffet, K.; Gillon, E.; Holler, M.; Nierengarten, J.-F.; Imberty, A.; Vincent, S. P., Fucofullerenes as tight ligands of RSL and LecB, two bacterial lectins. *Organic & Biomolecular Chemistry* **2015**, *13* (23), 6482-6492.
69. Nierengarten, J. F., Fullerene hexa-adduct scaffolding for the construction of giant molecules. *Chemical Communications* **2017**, *53* (87), 11855-11868.
70. Cecioni, S.; Imberty, A.; Vidal, S., Glycomimetics versus Multivalent Glycoconjugates for the Design of High Affinity Lectin Ligands. *Chem Rev* **2015**, *115* (1), 525-561.
71. Buffet, K.; Nierengarten, I.; Galanos, N.; Gillon, E.; Holler, M.; Imberty, A.; Matthews, S. E.; Vidal, S.; Vincent, S. P.; Nierengarten, J.-F., Pillar[5]arene-Based Glycoclusters: Synthesis and Multivalent Binding to Pathogenic Bacterial Lectins. *Chemistry – A European Journal* **2016**, *22* (9), 2955-2963.
72. Galanos, N.; Gillon, E.; Imberty, A.; Matthews, S. E.; Vidal, S., Pentavalent pillar[5]arene-based glycoclusters and their multivalent binding to pathogenic bacterial lectins. *Organic & Biomolecular Chemistry* **2016**, *14* (13), 3476-3481.
73. Serda, M.; Malarz, K.; Mrozek-Wilczkiewicz, A.; Wojtyniak, M.; Musioł, R.; Curley, S. A., Glycofullerenes as non-receptor tyrosine kinase inhibitors- towards better nanotherapeutics for pancreatic cancer treatment. *Scientific reports* **2020**, *10* (1), 260-260.
74. Serda, M.; Ware, M. J.; Newton, J. M.; Sachdeva, S.; Krzykawska-Serda, M.; Nguyen, L.; Law, J.; Anderson, A. O.; Curley, S. A.; Wilson, L. J.; Corr, S. J., Development of photoactive Sweet-C(60) for pancreatic cancer stellate cell therapy. *Nanomedicine (Lond)* **2018**, *13* (23), 2981-2993.
75. Bartelmess, J.; Quinn, S. J.; Giordani, S., Carbon nanomaterials: multi-functional agents for biomedical fluorescence and Raman imaging. *Chem Soc Rev* **2015**, *44* (14), 4672-4698.
76. Baptista, F. R.; Belhout, S. A.; Giordani, S.; Quinn, S. J., Recent developments in carbon nanomaterial sensors. *Chem Soc Rev* **2015**, *44* (13), 4433-4453.
77. Liu, H.; Zhang, L.; Yan, M.; Yu, J., Carbon nanostructures in biology and medicine. *J. Mater. Chem. B* **2017**, *5* (32), 6437-6450.
78. Benzigar, M. R.; Talapaneni, S. N.; Joseph, S.; Ramadass, K.; Singh, G.; Scaranto, J.; Ravon, U.; Al-Bahily, K.; Vinu, A., Recent advances in functionalized micro and mesoporous carbon materials: synthesis and applications. *Chem Soc Rev* **2018**, *47* (8), 2680-2721.
79. Kwon, O. S.; Song, H. S.; Park, T. H.; Jang, J., Conducting Nanomaterial Sensor Using Natural Receptors. *Chem Rev* **2019**, *119* (1), 36-93.
80. Ibrahim, K. S., Carbon nanotubes-properties and applications: a review. *Carbon Letters* **2013**, *14*, 131-134.
81. Kong, N.; Shimpi, M. R.; Park, J. H.; Ramström, O.; Yan, M., Carbohydrate conjugation through microwave-assisted functionalization of single-walled carbon nanotubes using perfluorophenyl azides. *Carbohydr. Res.* **2015**, *405*, 33-38.
82. Dinesh, B.; Bianco, A.; Ménard-Moyon, C., Designing multimodal carbon nanotubes by covalent multi-functionalization. *Nanoscale* **2016**, *8* (44), 18596-18611.
83. Mallakpour, S.; Soltanian, S., Surface functionalization of carbon nanotubes: fabrication and applications. *RSC Advances* **2016**, *6* (111), 109916-109935.

84. Alshehri, R.; Ilyas, A. M.; Hasan, A.; Arnaout, A.; Ahmed, F.; Memic, A., Carbon Nanotubes in Biomedical Applications: Factors, Mechanisms, and Remedies of Toxicity. *Journal of Medicinal Chemistry* **2016**, *59* (18), 8149-8167.
85. Pernía Leal, M.; Assali, M.; Cid, J. J.; Valdivia, V.; Franco, J. M.; Fernández, I.; Pozo, D.; Khiar, N., Synthesis of 1D-glyconanomaterials by a hybrid noncovalent–covalent functionalization of single wall carbon nanotubes: a study of their selective interactions with lectins and with live cells. *Nanoscale* **2015**, *7* (45), 19259-19272.
86. Hussain, S.; Ji, Z.; Taylor, A. J.; DeGraff, L. M.; George, M.; Tucker, C. J.; Chang, C. H.; Li, R.; Bonner, J. C.; Garantziotis, S., Multiwalled Carbon Nanotube Functionalization with High Molecular Weight Hyaluronan Significantly Reduces Pulmonary Injury. *ACS Nano* **2016**, *10* (8), 7675-7688.
87. Dosekova, E.; Filip, J.; Bertok, T.; Both, P.; Kasak, P.; Tkac, J., Nanotechnology in Glycomics: Applications in Diagnostics, Therapy, Imaging, and Separation Processes. *Med Res Rev* **2017**, *37* (3), 514-626.
88. Kasprzak, A.; Poplawska, M., Recent developments in the synthesis and applications of graphene-family materials functionalized with cyclodextrins. *Chemical Communications* **2018**, *54* (62), 8547-8562.
89. Nazarzadeh Zare, E.; Makvandi, P.; Borzacchiello, A.; Tay, F. R.; Ashtari, B.; V. T. Padil, V., Antimicrobial gum bio-based nanocomposites and their industrial and biomedical applications. *Chemical Communications* **2019**, *55* (99), 14871-14885.
90. Dong, Z.; Wang, Q.; Huo, M.; Zhang, N.; Li, B.; Li, H.; Xu, Y.; Chen, M.; Hong, H.; Wang, Y., Mannose-Modified Multi-Walled Carbon Nanotubes as a Delivery Nanovector Optimizing the Antigen Presentation of Dendritic Cells. *ChemistryOpen* **2019**, *8* (7), 915-921.
91. Rodríguez-Pérez, L.; Ramos-Soriano, J.; Pérez-Sánchez, A.; Illescas, B. M.; Muñoz, A.; Luczkowiak, J.; Lasala, F.; Rojo, J.; Delgado, R.; Martín, N., Nanocarbon-Based Glycoconjugates as Multivalent Inhibitors of Ebola Virus Infection. *Journal of the American Chemical Society* **2018**, *140* (31), 9891-9898.
92. Cid Martín, J. J.; Assali, M.; Fernández-García, E.; Valdivia, V.; Sánchez-Fernández, E. M.; Garcia Fernández, J. M.; Wellinger, R. E.; Fernández, I.; Khiar, N., Tuning of glyconanomaterial shape and size for selective bacterial cell agglutination. *J. Mater. Chem. B* **2016**, *4* (11), 2028-2037.
93. Pramanik, A.; Jones, S.; Gao, Y.; Sweet, C.; Begum, S.; Shukla, M. K.; Buchanan, J. P.; Moser, R. D.; Ray, P. C., A bio-conjugated chitosan wrapped CNT based 3D nanoporous architecture for separation and inactivation of Rotavirus and Shigella waterborne pathogens. *J. Mater. Chem. B* **2017**, *5* (48), 9522-9531.
94. Romero-Ben, E.; Cid, J. J.; Assali, M.; Fernández-García, E.; Wellinger, R. E.; Khiar, N., Surface modulation of single-walled carbon nanotubes for selective bacterial cell agglutination. *Int J Nanomedicine* **2019**, *14*, 3245-3263.
95. Datir, S. R.; Das, M.; Singh, R. P.; Jain, S., Hyaluronate Tethered, “Smart” Multiwalled Carbon Nanotubes for Tumor-Targeted Delivery of Doxorubicin. *Bioconjugate Chemistry* **2012**, *23* (11), 2201-2213.
96. Hou, L.; Zhang, H.; Wang, Y.; Wang, L.; Yang, X.; Zhang, Z., Hyaluronic acid-functionalized single-walled carbon nanotubes as tumor-targeting MRI contrast agent. *Int J Nanomedicine* **2015**, *10*, 4507-4520.
97. Cao, X.; Tao, L.; Wen, S.; Hou, W.; Shi, X., Hyaluronic acid-modified multiwalled carbon nanotubes for targeted delivery of doxorubicin into cancer cells. *Carbohydr. Res.* **2015**, *405*, 70-77.
98. Arosio, P.; Comito, G.; Orsini, F.; Lascialfari, A.; Chiarugi, P.; Ménard-Moyon, C.; Nativi, C.; Richichi, B., Conjugation of a GM3 lactone mimetic on carbon nanotubes enhances the related inhibition of melanoma-associated metastatic events. *Organic & Biomolecular Chemistry* **2018**, *16* (33), 6086-6095.
99. Hummers, W. S.; Offeman, R. E., Preparation of Graphitic Oxide. *Journal of the American Chemical Society* **1958**, *80* (6), 1339-1339.

100. Tarcan, R.; Todor-Boer, O.; Petrovai, I.; Leordean, C.; Astilean, S.; Botiz, I., Reduced graphene oxide today. *Journal of Materials Chemistry C* **2020**, *8* (4), 1198-1224.
101. Cheng, C.; Li, S.; Thomas, A.; Kotov, N. A.; Haag, R., Functional Graphene Nanomaterials Based Architectures: Biointeractions, Fabrications, and Emerging Biological Applications. *Chem Rev* **2017**, *117* (3), 1826-1914.
102. Priyadarsini, S.; Mohanty, S.; Mukherjee, S.; Basu, S.; Mishra, M., Graphene and graphene oxide as nanomaterials for medicine and biology application. *Journal of Nanostructure in Chemistry* **2018**, *8* (2), 123-137.
103. Ruhl, G.; Wittmann, S.; Koenig, M.; Neumaier, D., The integration of graphene into microelectronic devices. *Beilstein Journal of Nanotechnology* **2017**, *8* (1), 1056-1064.
104. Akinwande, D.; Kireev, D., Wearable graphene sensors use ambient light to monitor health. *Nature* **2019**, *576* (7786), 220-221.
105. Kong, N.; Park, J.; Yang, X.; Ramström, O.; Yan, M., Carbohydrate Functionalization of Few-Layer Graphene through Microwave-Assisted Reaction of Perfluorophenyl Azide. *ACS Applied Bio Materials* **2019**, *2* (1), 284-291.
106. Sharma, D.; Rao, N. N. M.; Arasaretnam, S.; Sessa Sainath, A. V.; Dhayal, M., Functionalization of structurally diverse glycopolymers on graphene oxide surfaces and their quantification through fluorescence resonance energy transfer with fluorescein isothiocyanate. *Colloid and Polymer Science* **2020**.
107. Sayyar, S.; Murray, E.; Gambhir, S.; Spinks, G.; Wallace, G. G.; Officer, D. L., Synthesis and Characterization of Covalently Linked Graphene/Chitosan Composites. *JOM* **2016**, *68* (1), 384-390.
108. Kim, J.; Lee, M.-S.; Jeon, S.; Kim, M.; Kim, S.; Kim, K.; Bien, F.; Hong, S. Y.; Park, J.-U., Highly transparent and stretchable field-effect transistor sensors using graphene-nanowire hybrid nanostructures. *Advanced materials* **2015**.
109. He, X.-P.; Zang, Y.; James, T. D.; Li, J.; Chen, G.-R.; Xie, J., Fluorescent glycoprobes: a sweet addition for improved sensing. *Chemical Communications* **2016**, *53* (1), 82-90.
110. Jiang, T.; Tan, H.; Sun, Y.; Wang, J.; Hang, Y.; Lu, N.; Yang, J.; Qu, X.; Hua, J., Graphene oxide-based NIR fluorescence probe with aggregation-induced emission property for lectins detection and liver cells targeting. *Sensors and Actuators B: Chemical* **2018**, *261*, 115-126.
111. He, X.-P.; Zhu, B.-W.; Zang, Y.; Li, J.; Chen, G.-R.; Tian, H.; Long, Y.-T., Dynamic tracking of pathogenic receptor expression of live cells using pyrenyl glycoanthraquinone-decorated graphene electrodes. *Chemical Science* **2015**, *6* (3), 1996-2001.
112. Xie, D.; Feng, X.-Q.; Hu, X.-L.; Liu, L.; Ye, Z.; Cao, J.; Chen, G.-R.; He, X.-P.; Long, Y.-T., Probing Mannose-Binding Proteins That Express on Live Cells and Pathogens with a Diffusion-to-Surface Ratiometric Graphene Electrosensor. *ACS Applied Materials & Interfaces* **2016**, *8* (38), 25137-25141.
113. He, X.-P.; Tian, H., Lightening Up Membrane Receptors with Fluorescent Molecular Probes and Supramolecular Materials. *Chem* **2018**, *4* (2), 246-268.
114. Ji, D.-K.; Chen, G.-R.; He, X.-P.; Tian, H., Simultaneous Detection of Diverse Glycoligand-Receptor Recognitions Using a Single-Excitation, Dual-Emission Graphene Composite. *Advanced Functional Materials* **2015**, *25* (23), 3483-3487.
115. Liu, S.; Zeng, T. H.; Hofmann, M.; Burcombe, E.; Wei, J.; Jiang, R.; Kong, J.; Chen, Y., Antibacterial Activity of Graphite, Graphite Oxide, Graphene Oxide, and Reduced Graphene Oxide: Membrane and Oxidative Stress. *ACS Nano* **2011**, *5* (9), 6971-6980.
116. Chandler, C. I. R., Current accounts of antimicrobial resistance: stabilisation, individualisation and antibiotics as infrastructure. *Palgrave Communications* **2019**, *5* (1), 1-13.
117. Kumar, P.; Huo, P.; Zhang, R.; Liu, B., Antibacterial Properties of Graphene-Based Nanomaterials. *Nanomaterials* **2019**, *9* (5), 737.
118. Szunerits, S.; Boukherroub, R., Antibacterial activity of graphene-based materials. *J. Mater. Chem. B* **2016**, *4* (43), 6892-6912.

119. Nizet, V.; Varki, A.; Aebi, M., Microbial Lectins: Hemagglutinins, Adhesins, and Toxins. In *Essentials of Glycobiology*, Varki, A.; Cummings, R. D.; Esko, J. D.; Stanley, P.; Hart, G. W.; Aebi, M.; Darvill, A. G.; Kinoshita, T.; Packer, N. H.; Prestegard, J. H.; Schnaar, R. L.; Seeberger, P. H., Eds. Cold Spring Harbor Laboratory Press

Copyright 2015-2017 by The Consortium of Glycobiology Editors, La Jolla, California. All rights reserved.: Cold Spring Harbor (NY), 2015; pp 481-91.

120. Khodadadi Chegeni, B.; Dadkhah Tehrani, A.; Adeli, M., Glyco-functionalized graphene oxides as green antibacterial absorbent materials. *Journal of the Taiwan Institute of Chemical Engineers* **2019**, *96*, 176-184.

121. Qi, Z.; Bharate, P.; Lai, C.-H.; Ziem, B.; Böttcher, C.; Schulz, A.; Beckert, F.; Hatting, B.; Mülhaupt, R.; Seeberger, P. H.; Haag, R., Multivalency at Interfaces: Supramolecular Carbohydrate-Functionalized Graphene Derivatives for Bacterial Capture, Release, and Disinfection. *Nano Letters* **2015**, *15* (9), 6051-6057.

122. Maruthupandy, M.; Rajivgandhi, G.; Muneeswaran, T.; Anand, M.; Quero, F., Highly efficient antibacterial activity of graphene/chitosan/magnetite nanocomposites against ESBL-producing *Pseudomonas aeruginosa* and *Klebsiella pneumoniae*. *Colloids and Surfaces B: Biointerfaces* **2021**, *202*, 111690.

123. Shende, P.; Pathan, N., Potential of carbohydrate-conjugated graphene assemblies in biomedical applications. *Carbohydrate Polymers* **2021**, *255*, 117385.

124. Rostami, S.; Puza, F.; Ucak, M.; Ozgur, E.; Gul, O.; Ercan, U. K.; Garipcan, B., Bifunctional sharkskin mimicked chitosan/graphene oxide membranes: Reduced biofilm formation and improved cytocompatibility. *Applied Surface Science* **2021**, *544*, 148828.

125. Rahnamaee, S. Y.; Bagheri, R.; Heidarpour, H.; Vossoughi, M.; Golizadeh, M.; Samadikuchaksaraei, A., Nanofibrillated chitosan coated highly ordered titania nanotubes array/graphene nanocomposite with improved biological characters. *Carbohydrate Polymers* **2021**, *254*, 117465.

126. Diaz-Galvez, K. R.; Teran-Saavedra, N. G.; Burgara-Estrella, A. J.; Fernandez-Quiroz, D.; Silva-Campa, E.; Acosta-Elias, M.; Sarabia-Sainz, H. M.; Pedroza-Montero, M. R.; Sarabia-Sainz, J. A., Specific capture of glycosylated graphene oxide by an asialoglycoprotein receptor: a strategic approach for liver-targeting. *RSC Advances* **2019**, *9* (18), 9899-9906.

127. Ji, D.-K.; Zhang, Y.; Zang, Y.; Liu, W.; Zhang, X.; Li, J.; Chen, G.-R.; James, T. D.; He, X.-P., Receptor-targeting fluorescence imaging and theranostics using a graphene oxide based supramolecular glycocomposite. *J. Mater. Chem. B* **2015**, *3* (47), 9182-9185.

128. Wang, C.; Zhang, Z.; Chen, B.; Gu, L.; Li, Y.; Yu, S., Design and evaluation of galactosylated chitosan/graphene oxide nanoparticles as a drug delivery system. *Journal of Colloid and Interface Science* **2018**, *516*, 332-341.

129. de Sousa, M.; Martins, C. H. Z.; Franqui, L. S.; Fonseca, L. C.; Delite, F. S.; Lanzoni, E. M.; Martinez, D. S. T.; Alves, O. L., Covalent functionalization of graphene oxide with d -mannose: evaluating the hemolytic effect and protein corona formation. *J. Mater. Chem. B* **2018**, *6* (18), 2803-2812.

130. Oh, B.; Lee, C. H., Development of Man-rGO for Targeted Eradication of Macrophage Ablation. *Molecular Pharmaceutics* **2015**, *12* (9), 3226-3236.

131. Lima-Sousa, R.; de Melo-Diogo, D.; Alves, C. G.; Costa, E. C.; Ferreira, P.; Louro, R. O.; Correia, I. J., Hyaluronic acid functionalized green reduced graphene oxide for targeted cancer photothermal therapy. *Carbohydrate Polymers* **2018**, *200*, 93-99.

132. Kang, S.; Hong, Y. L.; Ku, B.-C.; Lee, S.; Ryu, S.; Min, D.-H.; Jang, H.; Kim, Y.-K., Synthesis of biologically-active reduced graphene oxide by using fucoidan as a multifunctional agent for combination cancer therapy. *Nanotechnology* **2018**, *29* (47), 475604.

133. Rosenblum, D.; Joshi, N.; Tao, W.; Karp, J. M.; Peer, D., Progress and challenges towards targeted delivery of cancer therapeutics. *Nat Commun* **2018**, *9*.

134. Liang, W.; Huang, Y.; Lu, D.; Ma, X.; Gong, T.; Cui, X.; Yu, B.; Yang, C.; Dong, C.; Shuang, S.,  $\beta$ -Cyclodextrin–Hyaluronic Acid Polymer Functionalized Magnetic Graphene Oxide Nanocomposites for Targeted Photo-Chemotherapy of Tumor Cells. *Polymers* **2019**, *11* (1), 133.
135. Yin, T.; Liu, J.; Zhao, Z.; Zhao, Y.; Dong, L.; Yang, M.; Zhou, J.; Huo, M., Redox Sensitive Hyaluronic Acid-Decorated Graphene Oxide for Photothermally Controlled Tumor-Cytoplasm-Selective Rapid Drug Delivery. *Advanced Functional Materials* **2017**, *27* (14), 1604620.
136. Hill, S.; Galan, M. C., Fluorescent carbon dots from mono- and polysaccharides: synthesis, properties and applications. *Beilstein J Org Chem* **2017**, *13*, 675-693.
137. Hill, S. A.; Benito-Alifonso, D.; Davis, S. A.; Morgan, D. J.; Berry, M.; Galan, M. C., Practical Three-Minute Synthesis of Acid-Coated Fluorescent Carbon Dots with Tuneable Core Structure. *Scientific Reports* **2018**, *8* (1), 12234.
138. Hill, S. A.; Benito-Alifonso, D.; Morgan, D. J.; Davis, S. A.; Berry, M.; Galan, M. C., Three-minute synthesis of sp<sup>3</sup> nanocrystalline carbon dots as non-toxic fluorescent platforms for intracellular delivery. *Nanoscale* **2016**, *8* (44), 18630-18634.
139. Hill, S. A.; Sheikh, S.; Zhang, Q.; Sueiro Ballesteros, L.; Herman, A.; Davis, S. A.; Morgan, D. J.; Berry, M.; Benito-Alifonso, D.; Galan, M. C., Selective photothermal killing of cancer cells using LED-activated nucleus targeting fluorescent carbon dots. *Nanoscale Adv.* **2019**, *1* (8), 2840-2846.
140. Swift, T. A.; Duchi, M.; Hill, S. A.; Benito-Alifonso, D.; Harniman, R. L.; Sheikh, S.; Davis, S. A.; Seddon, A. M.; Whitney, H. M.; Galan, M. C.; Oliver, T. A. A., Surface functionalisation significantly changes the physical and electronic properties of carbon nano-dots. *Nanoscale* **2018**, *10* (29), 13908-13912.
141. Swift, T. A.; Oliver, T. A. A.; Galan, M. C.; Whitney, H. M., Functional nanomaterials to augment photosynthesis: evidence and considerations for their responsible use in agricultural applications. *Interface Focus* **2019**, *9* (1), 20180048.